Inorganic Chemistry

Article

pubs.acs.org/IC

Toward the Understanding of Radical Reactions: Experimental and Computational Studies of Titanium(III) Diamine Bis(phenolate) Complexes

Sónia Barroso,[†] Filipe Madeira,[†] Maria José Calhorda,[‡] M. João Ferreira,[†] M. Teresa Duarte,[†] and Ana M. Martins*,[†]

[†]Centro de Química Estrutural, Instituto Superior Técnico, TU Lisbon, 1049-001 Lisboa, Portugal

[‡]Departamento de Química e Bioquímica, Faculdade de Ciências, Universidade de Lisboa, Campo Grande, Ed. C8, 1749-016 Lisboa, Portugal

Supporting Information

ABSTRACT: Radical reactions of titanium(III) [Ti(^{tBu2}O$_2$NN′)Cl(S)] (S = THF, **1**; S = py, **2**; ^{tBu2}O$_2$NN′ = Me$_2$N(CH$_2$)$_2$N(CH$_2$-2-O-3,5-^{t}Bu$_2$C$_6$H$_2$)$_2$) are described. Reactions with neutral electron acceptors led to metal oxidation to Ti(IV), [Ti(^{tBu2}O$_2$NN′)Cl(TEMPO)] (**4**) being formed with the TEMPO radical and [Ti(^{tBu2}O$_2$NN′)Cl$_2$] (**9**) with PhN═NPh. [Ti(^{tBu2}O$_2$NN′)Cl$_2$] was also formed when [Ti(^{tBu2}O$_2$NN′)Cl(S)] was oxidized by [Cp$_2$Fe][BPh$_4$], but the [Cp$_2$Fe][PF$_6$] analogue yielded [Ti(^{tBu2}O$_2$NN′)ClF] (**8**). The reactions of [Ti(^{tBu2}O$_2$NN′)Cl(S)] with O$_2$ gave [Ti(^{tBu2}O$_2$NN′)Cl]$_2$(μ-O) (**3**). The DFT calculated Gibbs energy for the above reaction showed it to be exergonic (ΔG_{298} = −123.6 kcal·mol^{-1}). [Ti(^{tBu2}O$_2$NN′)(CH$_2$Ph)(S)] (S = THF, **5**; py, **6**) are not stable in solution for long periods and in diethyl ether gave 1:1 cocrystals of [Ti(^{tBu2}O$_2$NN′)(CH$_2$Ph)$_2$] (**7**) and [Ti(^{tBu2}O$_2$NN′)Cl]$_2$(μ-O) (**3**), most probably resulting from a disproportionation process of titanium(III) followed by oxygen abstraction by the resulting Ti(II) species. The oxidation of [Ti(^{tBu2}O$_2$NN′)(κ^2-{CH$_2$-2-(NMe$_2$)-C$_6$H$_4$})] (**10**), which is a Ti(III) benzyl stabilized by the intramolecular coordination of the NMe$_2$ moiety, led to a complex mixture. Recrystallization of this mixture under air led to a 1:1 cocrystal of two coordination isomers of the titanium oxo dimer (**3**). In one of these isomers, one metal is pentacoordinate and the dimethylamine moiety of the diamine bis(phenolate) ligand is not bonded to the metal, displaying a coordination mode of the ligand never observed before. The other titanium center is distorted octahedral with two *cis*-phenolate moieties. In the second unit, the coordination of the two ancillary ligands to the titanium centers reveals mutually *cis*-phenolate groups in one-half of the molecule and *trans*-coordinated in the other titanium center, keeping a distorted octahedral environment around each titanium.

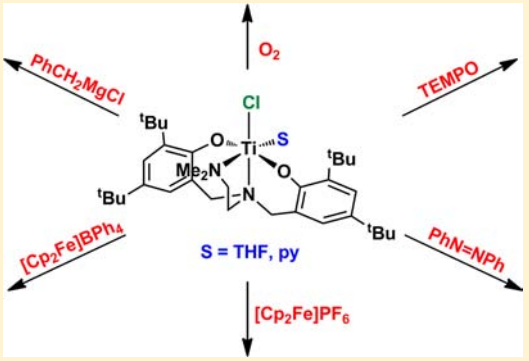

INTRODUCTION

A variety of structural architectures based on the combination of hard phenolate donors with neutral 2e donors were shown to stabilize early transition metal and lanthanide complexes.[1] The strong interactions established by the phenolate moieties with those electrophilic metals, in combination with one or two amine fragments incorporated in the ligand sets, give rise to well-defined monomeric transition metal compounds when bulky substituents occupy the *ortho*-phenolate positions.[2] The investigation of this class of compounds focused mainly on medicinal and catalytic applications.[3] Ti(IV) complexes of tetradentate diamine bis(phenolate) ligands revealed higher cytotoxic activity than that measured for cisplatin toward colon and ovarian tumor cells.[3b] Ti(IV) and Zr(IV) complexes of this type were also explored as catalysts of olefin polymerization and ROP of cyclic esters.[4] It was recently reported by Kol and co-workers that several Ti(IV) salalen-type complexes bearing chiral moieties exhibit high activity in polymerization of 1-propylene with very high isotacticities (>99% of isotactic polypropylene achieved for the catalyst with an adamanthyl substituent).[5] Moreover, the very narrow molecular weight distributions are in agreement with the living nature of the polymerization. Ti(IV) and Zr(IV) complexes with dianionic and trianionic amine-phenolate type ligands, including the tripodal ones, have also shown satisfactory results in ROP of *L*-lactide.[6] Again, the relatively narrow polydispersity index values obtained for isotactic polylactide indicate living polymerization systems.

We have recently explored the chemistry of tripodal diamine (bis)phenolate complexes in oxidation catalysis and showed that vanadium compounds are extremely active and selective in the sulfoxidation of thioethers.[7] Furthermore, we described M(III) complexes of general formula [M(^{tBu2}O$_2$NN′)Cl(S)] (M = Ti, Y; ^{tBu2}O$_2$NN′ = Me$_2$N(CH$_2$)$_2$N(CH$_2$-2-OH-3,5-^{t}Bu$_2$C$_6$H$_2$)$_2$; S = THF, DME) and reported preliminary studies of their reactivity.[8]

Received: April 23, 2013
Published: August 8, 2013

   dx.doi.org/10.1021/ic401008y | *Inorg. Chem.* 2013, 52, 9427−9439

Scheme 1

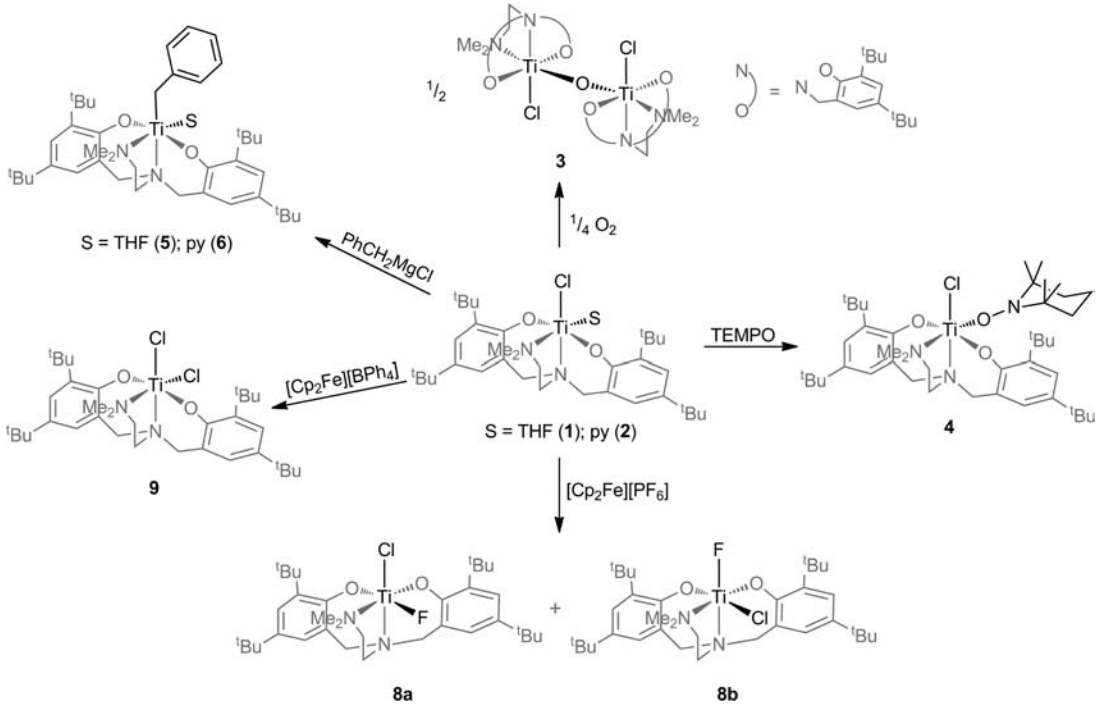

As part of this program, we report now further reactions that reveal new reactivity patterns of Ti(III) complexes supported by the tripodal $^{tBu2}O_2NN'$ donor set.

The significance of Ti(III) complexes in organic syntheses is largely documented.[9] Pinacol and McMurry reactions as well as the opening of strained rings, with particular emphasis on epoxides, are powerful methods for constructing organic molecules that are often not accessible by other methods.[10] These reactions often suffer from reproducibility problems intrinsic to the substrates or the reduced titanium species that are commonly generated *in situ*, by the addition of reducing agents to titanium(IV) precursors.

Up to now, the stabilization of Ti(III) complexes was mainly based on biscyclopentadienyl motifs,[11] and beyond those, only a few titanium(III) complexes with silox and triamidoamine ancillary ligands were reported.[12] Taking into account the successful applications of diamine bis(phenolate) metal complexes, it is surprising that paramagnetic transition metal species of this family remain essentially unexplored. We report here electron-transfer reactions mediated by [Ti($^{tBu2}O_2NN'$)Cl(S)] and DFT calculations that complement and clarify its reaction with O_2. This work is thus a contribution to the broadening and improved understanding of the reactivity of paramagnetic titanium compounds that is central for the development of useful applications.

RESULTS AND DISCUSSION

Chemical Studies. As previously reported, [Ti($^{tBu2}O_2NN'$)-Cl(THF)] (**1**; $^{tBu2}O_2NN' = Me_2N(CH_2)_2N(CH_2\text{-}2\text{-}OH\text{-}3,5\text{-}{}^tBu_2C_6H_2)_2$) is readily prepared by treatment of [$TiCl_3(THF)_3$] with $Na_2(^{tBu2}O_2NN')$ in THF. The addition of pyridine to a solution of **1** leads to THF replacement and the formation of [Ti($^{tBu2}O_2NN'$)Cl(py)] (**2**).[8] Reactions of **1** or **2** with oxygen, carried out in THF solutions by allowing the slow diffusion of air over a column of anhydrous $CaCl_2$, gave rise to the formation of the oxo-bridged dimer [Ti($^{tBu2}O_2NN'$)Cl]$_2$(μ-O) (**3**), in high yield (Scheme 1). [Ti($^{tBu2}O_2NN'$)Cl]$_2$(μ-O) is a very stable complex, not susceptible to hydrolysis in the air. The ^{1}H NMR spectrum of **3** in C_6D_6 exhibits two doublets ($^4J_{HH}$ = 2.2 Hz) for the aromatic protons, two singlets for the *tert*-butyl groups, two multiplets for the protons of the C_2 chain linked to the tripodal nitrogen, one singlet for the CH_3 protons of the dimethylamine fragment, and one AX system (at δ = 5.77 and 3.30 ppm) assigned to the methylene protons of the $NCH_2{}^{tBu2}PhO$ groups. This pattern points out a rigid chelation on the NMR time scale, consistent with C_{2v} symmetry, with mutually *trans*-phenolate groups. The molecular structure of **3** determined by single crystal X-ray diffraction confirms this pattern. An ORTEP drawing of the structure of **3** is shown in Figure 1, and relevant bond lengths and angles are displayed in Table 1.

The structure features an oxygen-bridged dinuclear titanium-(IV) complex with slightly distorted octahedral geometry around each metal center. The equatorial planes are defined by O1, O2, and N2 of the diamine bis(phenolate) ligands and the bridging oxygen O3, while the axial positions are occupied by the tripodal nitrogens N1 and the chloride ligands Cl1. The two sides of the molecule are structurally related across a linear oxo bridge by a rotation of 180°. In each titanium center, the bridging oxygen and the chloride ligand occupy *cis* positions. The phenolate groups present *trans*-coordination with a dihedral angle of 154.2(1)° between them. The bond distances and angles are within the expected ranges for titanium(IV) complexes.[13] The linearity of the Ti−O−Ti fragment is in agreement with a Ti−O multiple bond with a significant π contribution from the oxygen. The Ti−(μ-O) distance and the Ti−(μ-O)−Ti angle compare well with values reported for other linear oxo bridged titanium(IV) complexes such as [Ti($^{tBu2}O_2NN'$)(OEt)]$_2$−(μ-O).[14] The Ti1−N2 bond length is longer than Ti1−N1 owing to the *trans* influence of the μ-oxo group.

Compounds containing the Ti−O−Ti core are commonly obtained by controlled hydrolysis of Ti−X bonds (X = halide, alkyl) of Ti(IV) complexes, but in view of the high oxophilicity of

dx.doi.org/10.1021/ic401008y | *Inorg. Chem.* 2013, 52, 9427−9439

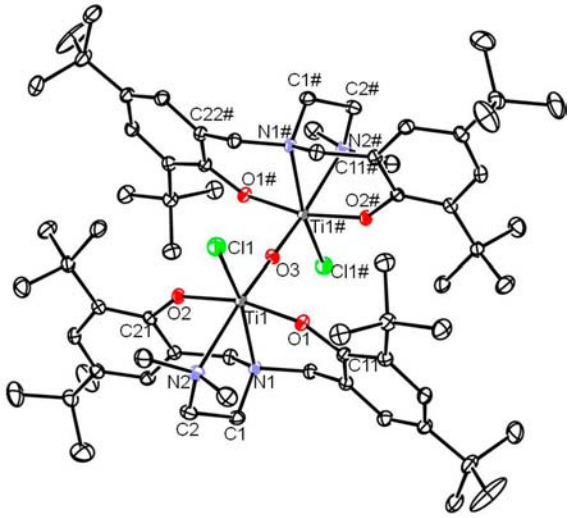

Figure 1. ORTEP-3 diagram of $[Ti(^{tBu2}O_2NN')Cl]_2(\mu\text{-}O)$ (**3**), using 40% probability level ellipsoids. The equivalent atoms labeled with # are generated using the symmetry transformation $-x + 1, -y + 1, -z$. Hydrogen atoms are omitted for clarity.

Table 1. Selected Structural Parameters for 3, 4, 8, and 9

	3	4	8	9
		distances (Å)		
Ti1−O1	1.869(1)	1.894(3)	1.818(2)	1.842(2)
Ti1−O2	1.861(1)	1.887(3)	1.832(2)	1.833(2)
Ti1−X[a]	1.820(1)	1.783(3)	1.861(1)	2.320(1)
Ti1−N1	2.246(2)	2.228(4)	2.243(2)	2.254(2)
Ti1−N2	2.422(2)	2.441(4)	2.297(2)	2.291(3)
Ti1−Cl1	2.322(1)	2.345(1)	2.289(1)	2.304(1)
N3−O3		1.407(5)		
Ti1-eq. plane[b]	0.184(1)	0.154(2)	0.251(1)	0.191(1)
		angles (deg)		
O1−Ti1−O2	166.1(1)	165.6(1)	95.0(1)	167.8(1)
O1−Ti1−X	95.2(1)	95.1(1)	91.1(1)	90.2(1)
O1−Ti1−N1	84.0(1)	84.9(1)	82.0(1)	84.5(1)
O1−Ti1−N2	87.1(1)	82.7(1)	158.8(1)	86.9(1)
O1−Ti1−Cl1	92.3(1)	93.8(1)	106.3(1)	97.5(1)
O2−Ti1−X	93.5(1)	95.6(1)	167.5(1)	90.5(1)
O2−Ti1−N1	84.9(1)	84.5(1)	84.1(1)	83.2(1)
O2−Ti1−N2	82.1(1)	85.2(1)	90.9(1)	90.5(1)
O2−Ti1−Cl1	96.0(1)	93.5(1)	93.2(1)	94.4(1)
N1−Ti1−X	92.6(1)	95.0(1)	86.0(1)	91.9(1)
N2−Ti1−X	167.8(1)	170.7(1)	79.7(1)	170.4(1)
N2−Ti1−Cl1	87.7(1)	87.9(1)	93.6(1)	87.9(1)
N1−Ti1−N2	75.7(1)	75.8(1)	78.3(1)	78.7(1)
N1−Ti1−Cl1	163.1(1)	163.7(1)	171.5(1)	166.4(1)
X−Ti1−Cl1	104.1(0)	101.3(1)	95.6(1)	101.5(0)
Ti1−O1−C11	143.0(1)	142.9(3)	135.4(2)	145.6(2)
Ti1−O2−C21	144.0(1)	142.3(3)	145.3(2)	146.0(2)
Ti(1)−O3−Ti(1)#	180.0			
Ti(1)−O3−N3		174.1(3)		
θ[c]	154.2(1)	153.4(2)	112.4(1)	176.8(2)

[a]X = O3 (**3**, **4**); F1 (**8**); Cl2 (**9**). [b]The equatorial plane is defined by atoms O1, O2, O3, and N2. [c]θ is the dihedral angle between the planes containing the phenolate rings.

titanium and the variety of oxygen bonding patterns, these species may present an array of assemblies that depend on the ancillary ligands.[14,15] Reactions of Ti(III) species with O_2, which is itself a diradical, are exceptionally favored; yet the isolation of titanium peroxo species by binding of oxygen between two titanium centers remains elusive.[16] This type of intermediate, which is significant in the context of dioxygen reduction,[17] was claimed to form on the TiO_2 surface along the process of photo-induced water oxidation[18] and was characterized for copper as *trans*-M−O−O−M by X-ray diffraction.[19] On the other hand, instead of the corresponding peroxo complexes, the reactions of [Ti(acen)Cl(THF)] (acen = N,N′-ethylenebis-(acetylacetoneiminate) dianion) or $[TiH(ArO)_3(PMe_3)]$ (ArO = 2,6-$^{i}Pr_2$PhO) with O_2 produce $[Ti(acen)Cl]_2(\mu\text{-}O)$ and $[Ti(OAr)_3]_2(\mu\text{-}O)$, respectively.[20] The thermal instability and great oxidation power of titanium peroxides[21] may be responsible for the restricted number of structurally characterized titanium peroxides.[22] The formation of the Ti−O−Ti core from putative M−O−O−M species formed from reactions of Ti(III) with O_2 may be envisaged as the one electron oxidation of Ti(III) by titanium peroxides as shown in Scheme 2. The

Scheme 2

thermodynamics of the formation of $[Ti(^{tBu2}O_2NN')Cl]_2(\mu\text{-}O)$ (**3**) from $[Ti(^{tBu2}O_2NN')Cl]_2(\mu\text{-}O_2)$ was studied by means of DFT calculations (see below).

Treatment of $[Ti(^{tBu2}O_2NN')Cl(THF)]$ (**1**) with the nitroxyl radical TEMPO (2,2,6,6-tetramethylpiperidine-1-oxyl) proceeded with radical coupling between titanium and TEMPO and resulted in the formal reduction of the latter and metal oxidation to titanium(IV). $[Ti(^{tBu2}O_2NN')Cl(TEMPO)]$ (**4**) was isolated as a red/orange crystalline solid in quantitative yield (Scheme 1). The ^{1}H and ^{13}C NMR spectra of **4** in C_6D_6 revealed only one resonance for the methyl groups of TEMPO, in agreement with κ^1-bonding to the titanium in a complex of C_s symmetry.[23] The pattern observed for the diamine bis-(phenolate) ligand in the ^{1}H NMR spectrum is analogous to the one described above for **3**, and the NOESY spectrum shows cross peaks between the *tert*-butyl groups in the *ortho*-phenolate positions and the dimethylamine group of the ancillary ligand, corroborating static κ^4-O_2NN' coordination to the titanium on the NMR time scale. Cross peaks between the *ortho*-phenolate substituents and the methyl groups of TEMPO further attest the bonding of the latter to titanium.

The structure of **4**, depicted in Figure 2, was confirmed by X-ray diffraction. Relevant bond lengths and angles are displayed in Table 1. The titanium coordination geometry is once again distorted octahedral and the *trans*-phenolate groups determine the C_s symmetry observed in solution by NMR. The six-membered ring of the TEMPO ligand is in the chair conformation. The N1−O3 bond length of 1.407(5) Å confirms the κ^1-binding mode of TEMPO, consistent with an anionic ligand.[23] The short Ti1−O3 bond distance of 1.783(3) Å and large Ti1−O3−N3 angle of 174.1(3)° suggest a strong O−Ti pπ−dπ interaction,[24] also in agreement with the reduction of the TEMPO radical by titanium. This strong interaction is responsible for the elongation of the Ti1−N2 bond *trans* to the TEMPO oxygen. Despite the multiple character of the Ti−O bond, the NMR spectra do not reveal constraints to the rotation around this bond in solution at room temperature.

dx.doi.org/10.1021/ic401008y | Inorg. Chem. 2013, 52, 9427−9439

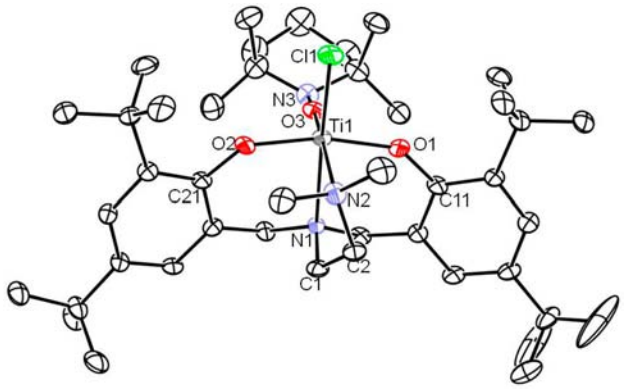

Figure 2. ORTEP-3 diagram of [Ti(^{tBu2}O$_2$NN′)Cl(TEMPO)] (**4**), using 40% probability level ellipsoids. Hydrogen atoms are omitted for clarity.

The Ti−O bonding energy in Ti(TEMPO) complexes, which is a critical parameter in the homolytic cleavage of Ti−O bonds, may be readily modulated by the donor ability of the ancillary ligands.[25] Increasing the electron density at the metal, by increasing the number of cyclopentadienyl ligands along the series TiCp$_n$Cl$_{(3-n)}$(TEMPO) (n = 0, 1, 2), causes a significant decrease of the Ti−O bonding energy. In consequence, the biscyclopentadienyl complex behaves as a source of Ti(III) as it produces TiCp$_2$Cl and the nitroxyl radical upon thermal activation.[23b] In the case of **4**, the cleavage of the Ti−O bond does not lead to the parent Ti(III) complex but to [Ti(^{tBu2}O$_2$NN′)Cl]$_2$(μ-O) (**3**) that forms readily in CCl_4 or by standing for long periods in toluene solutions. This result reflects the poor electron donor properties of the diamine bis(phenolate) donor set in comparison to biscyclopentadienyl.[24,26]

Treatment of toluene solutions of **1** or **2** with one equivalent of PhCH$_2$MgCl in Et$_2$O gave the corresponding benzyl derivatives [Ti(^{tBu2}O$_2$NN′)(CH$_2$Ph)(S)] (S = THF, **5**; py, **6**), as shown in Scheme 1. The two compounds are identical with the exception of the neutral coligand (THF or py), but **6** was reproducibly isolated in higher yield than **5** (68% vs 44%) under the same experimental conditions. Both compounds are extremely sensitive, slowly decomposing in solution. Satisfactory elemental analysis was, however, obtained for [Ti(^{tBu2}O$_2$NN′)(CH$_2$Ph)(py)] (**6**), supporting its formulation as a solvent stabilized hexacoordinated species. On the other hand, the results of elemental analysis of **5** systematically deviated from the theoretical values, reflecting its extreme instability and decomposition under analytical experimental conditions. The description of both complexes as solvent adducts is further reinforced by the structures of the parent complexes and also of [Ti(^{tBu2}O$_2$NN′)-(κ^2-CH$_2$-2-NMe$_2$-C$_6$H$_4$)], which is stabilized by the coordination of the dimethylamine substituent on the *ortho* carbon of the benzyl ring.[8]

The EPR spectrum of **5** in toluene at 293 K exhibits two symmetrical single lines at g_1 = 1.951, corresponding to a major species, and at g_2 = 1.963, integrating to a minor compound. The main signal is attributed to [Ti(^{tBu2}O$_2$NN′)(CH$_2$Ph)(THF)], and the less intense signal is tentatively assigned to a pentacoordinated Ti(III) species resulting from THF dissociation. These data compare with those obtained for the parent complex [Ti(^{tBu2}O$_2$NN′)Cl(THF)] that displays a similar EPR spectrum with lines at g = 1.954 and g = 1.962.[8] The EPR spectrum of **6**, also obtained in toluene at 293 K, discloses only one symmetrical line with g = 1.952. As a whole, the results are in line with the higher instability of **5** relative to **6** and the weak bonding of THF in comparison with pyridine.

Attempts to obtain crystals of either **5** or **6** were unfruitful. Surprisingly, the analysis of the crystals obtained from an Et$_2$O solution of **6** by X-ray diffraction revealed the presence of two Ti(IV) species, [Ti(^{tBu2}O$_2$NN′)(CH$_2$Ph)$_2$] (**7**) and [Ti(^{tBu2}O$_2$NN′)Cl]$_2$(μ-O) (**3**), which cocrystallized in a 1:1 ratio (Figure 3). The cocrystal **3**·**7** displays half a molecule of **3** and one molecule of **7** in the asymmetric unit. The titanium dibenzyl complex **7** was previously synthesized by Kol and co-workers in a one-pot reaction from sequential addition of the ligand precursor, titanium tetra(isopropoxide), TMSCl, and PhCH$_2$MgCl.[2a] The structural parameters obtained for [Ti(^{tBu2}O$_2$NN′)-(CH$_2$Ph)$_2$] in the cocrystal **3**·**7** are in accordance with the data reported by Kol and co-workers. The data obtained for the molecule of **3** in the cocrystal are also in accordance with the data obtained for the single crystal of **3** described above.

The formation of the dibenzyl derivative **7** from [Ti(^{tBu2}O$_2$NN′)-(CH$_2$Ph)(py)] (**6**) may be assumed as resulting from the transfer of a benzyl radical between two molecules of **6**. The overall outcome of this exchange is the disproportionation of Ti(III) with formation

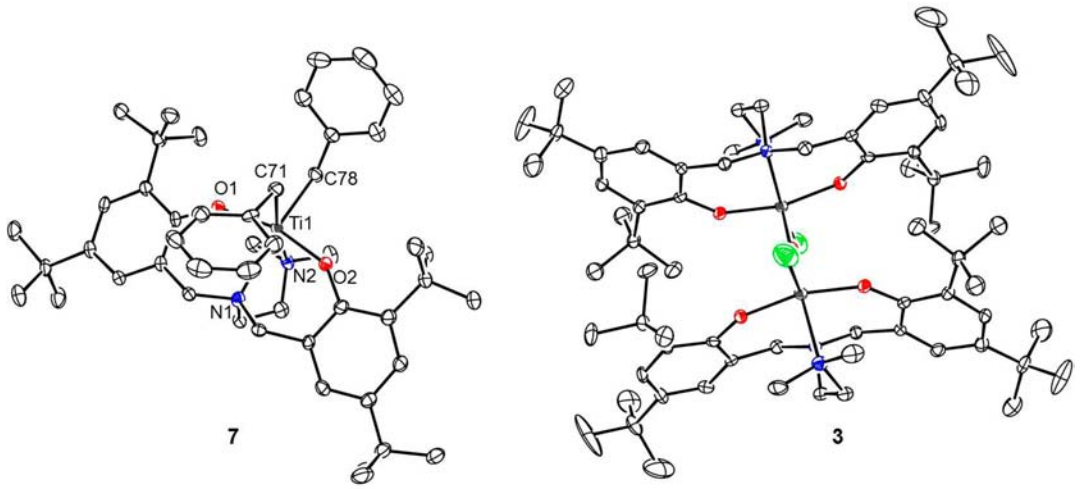

Figure 3. ORTEP-3 diagram of cocrystallized [Ti(^{tBu2}O$_2$NN′)(CH$_2$Ph)$_2$] and [Ti(^{tBu2}O$_2$NN′)Cl]$_2$(μ-O) (**3**·**7**), using 40% probability level ellipsoids. One half of **3** is generated using the symmetry transformation $-x + 1, -y + 1, -z$. Hydrogen atoms are omitted for clarity.

dx.doi.org/10.1021/ic401008y | *Inorg. Chem.* 2013, 52, 9427−9439

of the Ti(IV)dibenzyl species **7** and a hypothetical ($^{tBu2}O_2NN'$)-Ti(II) fragment that converts to **3** by abstracting oxygen and a chloride ligand.[27] The bridging oxo ligand may come from vestigial amounts of moisture or O_2, or the solvent. It is known from the literature that the strength of Ti═X bonds is an effective driving force for the reducing behavior displayed by Ti(II) complexes and that the high oxophilicity of reduced titanium complexes is responsible for particularly successful atom transfer reactions when X = O.[28] The source of the chloride ligand is uncertain, but it may possibly come from traces of $MgCl_2$ that did not separate completely during the extraction of [Ti($^{tBu2}O_2NN'$)(CH_2Ph)(py)] (**6**). It is known that removal of $MgCl_2$ upon alkylation reactions using Grignard reagents or reduction reactions with Mg is in some cases difficult.[29] Indeed, though the low solubility of $MgCl_2$ in organic solvents is a driving force for chloride metathesis, its removal from solution is often incomplete. The high affinity of magnesium for oxygen donors may be responsible for the binding and solubilization of $MgCl_2$, which is particularly effective when O-donor chelating ligands are present. Alternatively, it may be envisaged that a Ti(μ-Cl)MgCl core is present as a contaminant. Such types of situations may not be excluded and appear to be the most plausible explanations for the origin of the chloride ligand during the crystallization process. A related compound, presenting a bridging ^{i}PrO group between Ti(III) and one $Na(THF)_n^+$ cation, was previously reported and characterized by X-ray diffraction as [Ti{$Me_2NC_2H_4N(CH_2$-3,5-$^{t}Bu_2C_6H_2O$-2)$_2$}($O^{i}Pr$)$_2$Na$(THF)_2$].[30] Other examples of well characterized compounds displaying bridging chlorides between group 4 and representative metals have been reported.[31] Attempts to grow crystals from a solution of [Ti($^{tBu2}O_2NN'$)(CH_2Ph)(THF)] (**5**) after complete removal of $MgCl_2$ with dioxane were unproductive. Although a greenish microcrystalline solid formed from hexane solution after several weeks at −20 °C, the crystals and the mother solution turned orange at room temperature, and the proton NMR of this sample was inconclusive.

Reactions of [Ti($^{tBu2}O_2NN'$)Cl(S)] (S = THF, **1**; py, **2**) with [Cp_2Fe][X] (X = PF_6, BPh_4) showed that the diamine bis(phenolate) set is not efficient for the stabilization of the corresponding Ti(IV) cations. Fluoride abstraction and formation of [Ti($^{tBu2}O_2NN'$)ClF] (**8**) takes place in the presence of PF_6^-, while [Ti($^{tBu2}O_2NN'$)Cl_2] (**9**) is obtained in the presence of the noncoordinating BPh_4^- anion (Scheme 1). These results attest the extreme electrophilicity of the transient Ti(IV) cations that result from the 1:1 reaction of **1** with ferrocenium. It is likely that the abstraction of fluoride occurring in the presence of the PF_6^- anion is sustained by an inner sphere ion pair interaction [Ti($^{tBu2}O_2NN'$)Cl(FPF_5)] that evolves to [Ti($^{tBu2}O_2NN'$)ClF]. Similar processes involving acidic group 4 metal cations have been reported.[32] Contrary to all other complexes with $^{R2}O_2NN'$ ancillary ligands (R = Me, ^{t}Bu),[4a,7,8] **8** displays mutually *cis*-phenolate moieties that originate C_1-symmetry species. The isomerization process may proceed through the formation of a penta-coordinated trigonal bipyramidal intermediate, formed upon dissociation of THF/pyridine or the dimethylamine fragment. The origin of the isomerization process is likely determined by the bulkiness of the *tert*-butyl groups in the *ortho* positions of the phenolate groups that hinder the approach of the PF_6^- anion in the equatorial plane bisecting the O−Ti−O angle. Two isomers, **8a** and **8b**, are clearly detected in the ^{19}F NMR spectrum as two broad signals that integrate 6:1 at δ 122.5 ppm and 96.4 ppm. The presence of a second minor species of C_1 symmetry could also be detected by ^{1}H and ^{13}C NMR, although overlapping of most resonances was observed. VT NMR experiments run between −80 and 100 °C did not disclose the interconversion of the two species, which denotes the static coordination of the dimethyamine fragment after the formation of **8**. DFT calculations (see below) showed that a model of **8a**, with *tert*-buthyl groups replaced by methyls, is 3.5 kcal·mol^{-1} more stable than a similar model of **8b**. The small energy difference is in agreement with the NMR results. The molecular structure of **8a**, depicted in Figure 4, was further confirmed by

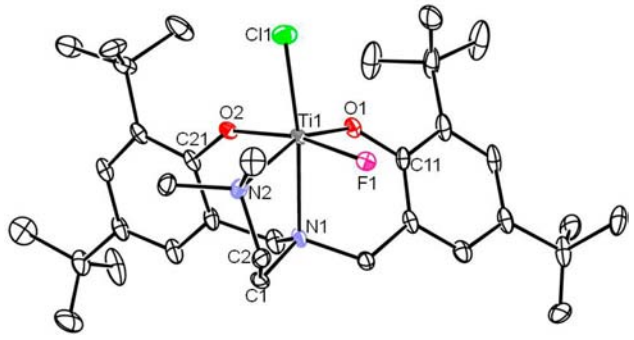

Figure 4. ORTEP-3 diagram of [Ti($^{tBu2}O_2NN'$)ClF] (**8a**), using 40% probability level ellipsoids. Hydrogen and disordered carbon atoms are omitted for clarity.

X-ray diffraction. Relevant bond lengths and angles are displayed in Table 1. The titanium coordination geometry is distorted octahedral, but the coordination mode of the diamine bis(phenolate) ligand to the titanium is different from that observed in the other complexes presented above. The two phenolate moieties are mutually *cis* with a dihedral angle of 112.4(1)° between the planes of the two rings. The Ti−F bond distance in **8** compares well with the values reported for titanium(IV) complexes displaying terminal Ti−F bonds, namely [Cp_2Ti(CF_3)F] and [{Cp*TiF(μ-F)(μ-OSO_2-*p*-$C_6H_4CH_3$)}$_2$] (Cp* = η^5-C_5Me_5).[33] As expected, the Ti−F bond length in **8** is much shorter than in [Ti_3(N═C$^{t}Bu_2$)$_6$(μ_2-F)$_3$((μ_3-F)$_2$][PF_6] despite the cationic nature of the latter complex.[32b] The high electronegativity of the fluoride ligand causes a more extensive pπ−dπ interaction between Ti1 and O2, as attested by the Ti1−O2−C21 angle that is 10° wider than Ti1−O1−C11.

In the reaction with [Cp_2Fe][BPh_4], the bulkiness of the BPh_4^- anion and its weak coordinating capabilities hamper the stabilization of [Ti($^{tBu2}O_2NN'$)Cl]$^+$ and give rise to the formation of [Ti($^{tBu2}O_2NN'$)Cl_2] (**9**) and other nonidentified decomposition products. Compound **9** was obtained as a crystalline material from Et_2O solution after sublimation of the ferrocene produced by the redox reaction. Hypothetically, the formation of [Ti($^{tBu2}O_2NN'$)Cl_2] may involve the cleavage of a dichloride bridged dication {[Ti($^{tBu2}O_2NN'$)]$_2$(μ-Cl)$_2$}$^{2+}$ that would originate the loss of at least 50% of titanium and would be responsible for the failure in the isolation of the envisaged cations. Orange crystals of **9** suitable for X-ray diffraction were grown from a C_6D_6 solution. The molecular structure of **9** is depicted in Figure 5, and relevant bond lengths and angles are displayed in Table 1. The titanium coordination geometry is distorted octahedral, with the two phenolate moieties *trans*-coordinated. The side arm fragment is coordinated to the metal, and the tripodal ligand forces the two chloride ligands to adopt mutually *cis* dispositions. The Ti−Cl distances compare well with the values reported for other titanium(IV) systems supported by O- and N-based ligands.[34] The wide Ti1−O1−C11 and

dx.doi.org/10.1021/ic401008y | Inorg. Chem. 2013, 52, 9427−9439

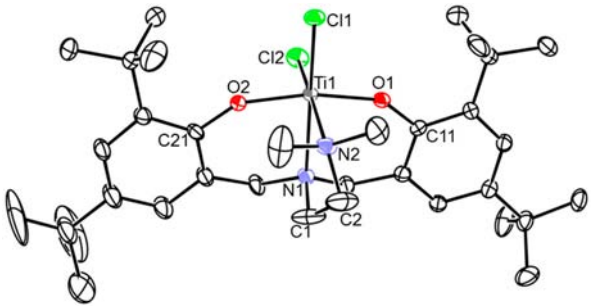

Figure 5. ORTEP-3 diagram of [Ti(^{tBu2}O$_2$NN′)Cl$_2$] (**9**), using 40% probability level ellipsoids. Hydrogen atoms are omitted for clarity.

Ti1−O2−C21 angles (145.6(2)° and 146.0(2)°, respectively) reflect some oxygen to metal pπ−dπ donation.

Attempts to reduce azobenzene by **1** also led to the isolation of a small amount of [Ti(^{tBu2}O$_2$NN′)Cl$_2$]. Although in a first instance this result might be surprising, it is in accordance with the reaction of **1** with [Cp$_2$Fe][BPh$_4$] described above. Once more, electron transfer should generate a Ti(IV) cation that is not stabilized by the azobenzene radical anion.

The oxidation of previously described [Ti(^{tBu2}O$_2$NN′)(κ^2-{CH$_2$-2-(NMe$_2$)-C$_6$H$_4$})] (**10**), prepared from the reaction of **1** with LiCH$_2$-2-(NMe$_2$)-C$_6$H$_4$ (Scheme 3),[8] was also attempted through reaction with [FeCp$_2$][PF$_6$]. The ^{1}H and ^{13}C NMR spectra of the red crystalline solid isolated after sublimation of the ferrocene formed are very complicated, revealing a mixture of compounds, and did not allow an unequivocal characterization. However, in C$_6$D$_6$, the ^{19}F NMR spectrum shows a doublet at δ = −70.69 ppm ($^1J_{FP}$ = 711 Hz), and the ^{31}P NMR spectrum displays a septet at δ = −143.0 ppm ($^1J_{PF}$ = 711 Hz), which attest to the presence of the PF_6^- anion and are consistent with the formation of a cationic species. If the compound [Ti(^{tBu2}O$_2$NN′)(κ^2-{CH$_2$-2-(NMe$_2$)-C$_6$H$_4$})][PF$_6$] would form in this reaction, the complexity of the NMR spectra might be related to the presence of isomers, the occurrence of fluxional processes, or even decomposition. All attempts to grow crystals of [Ti(^{tBu2}O$_2$NN′)(κ^2-{CH$_2$-2-(NMe$_2$)-C$_6$H$_4$})][PF$_6$] suitable for X-ray diffraction failed, but surprisingly, orange crystals grew from a Et$_2$O solution of the reaction mixture exposed to air. The analysis of the crystals revealed the formation of two cocrystallized coordination isomers (**11** and **12**) of [Ti(^{tBu2}O$_2$NN′)Cl]$_2$(μ-O) (**3**), as shown in Scheme 3.

An ORTEP view of cocrystal **11·12** is depicted in Figure 6. In **11**, the coordination geometry around the two titanium atoms is distorted octahedral, but the phenolate rings occupy *cis* positions in one metal center, while they are *trans*-coordinated in the other. In **12**, one of the titanium centers presents *cis*-phenolate moieties, and the NMe$_2$ fragment is coordinated to the metal defining a distorted octahedral geometry around the metal. In the second titanium center of **12**, the NMe$_2$ moiety is not coordinated to the metal, leading to a highly distorted trigonal bipyramidal geometry. Relevant bond lengths and angles for the cocrystal **11·12** can be found in the Supporting Information.

The chloride ligands in **11** and **12** probably arise from the lithium salt formed in the metathesis reaction that leads to [Ti(^{tBu2}O$_2$NN′)(κ^2-{CH$_2$-2-(NMe$_2$)-C$_6$H$_4$})]. The ubiquitous appearance of chloride ligands in the reactions described indicate that the alkaline metal salts are forming aggregates with the reaction products and are not efficiently removed by solvent extraction and filtration.[29] The different configurations of the phenolate groups found in **11·12** suggest that the formation of the cationic species may involve an isomerization process as the one observed in the formation of **8**. The dissociation of the dimethylamine fragment may originate a mixture of *cis*- and *trans*-phenolate arrangements that are responsible for the complex ^{1}H and ^{13}C NMR spectra already mentioned.

DFT Studies. Density functional theory calculations[35] (Gaussian 03/PBE1PBE,[36] see Computational Details) were performed in order to understand the origin of complexes **3** and **8** described above. Complex **1**, [Ti(^{tBu2}O$_2$NN′)Cl(THF)], loses THF in toluene solution, as revealed by EPR results, although [Ti(^{tBu2}O$_2$NN′)Cl] was not isolated.[8] Therefore, the model complex [Ti(^{Me2}O$_2$NN′)Cl] (**1***) was used as the starting compound for the calculations (Me was used instead of ^{t}Bu in all

Scheme 3

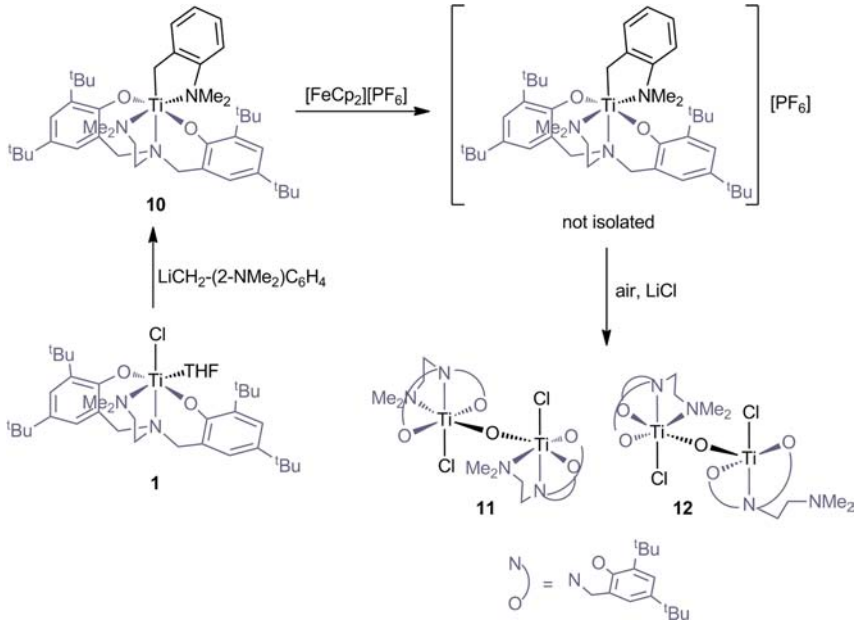

dx.doi.org/10.1021/ic401008y | Inorg. Chem. 2013, 52, 9427−9439

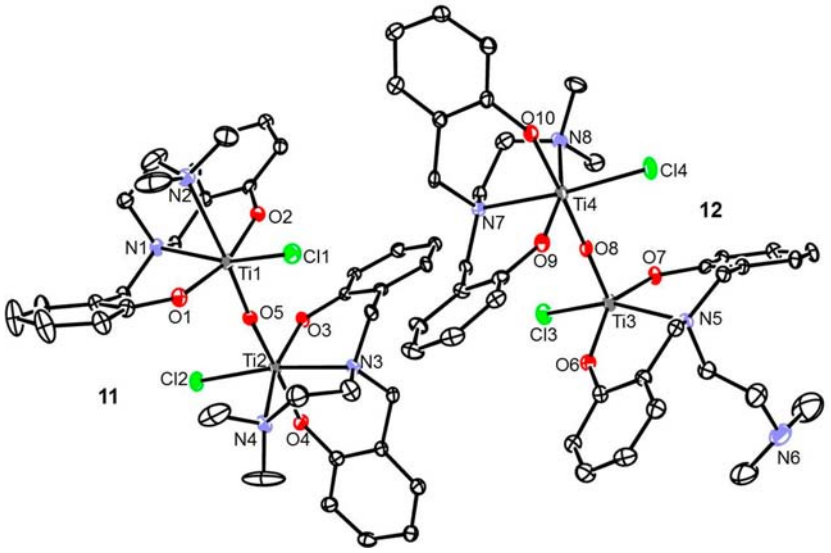

Figure 6. ORTEP-3 diagram of cocrystallized isomers of $[Ti(^{tBu2}O_2NN')Cl]_2(\mu\text{-}O)$ (**11**·**12**), using 30% probability level ellipsoids. Hydrogen atoms, *tert*-butyl groups, and disordered carbon atoms are omitted for clarity.

calculations). The formation of **1*** by dissociation of THF from **1** has been calculated as $\Delta G_{298} = -7.6$ kcal·mol^{-1}.

The Ti−O−Ti core of $[Ti(^{tBu2}O_2NN')Cl]_2(\mu\text{-}O)$ (**3**) formed in the reaction of $[Ti(^{tBu2}O_2NN')Cl]$ (**1***) with O_2 is proposed to result from the one electron oxidation of Ti(III) in **1** *via* a titanium peroxide species Ti−O−O−Ti (intermediate **B**). Therefore, it was considered that **1*** (Scheme 4) would react with O_2 to form a superoxide radical derivative (**A**), which reacts with a second equivalent of **1*** to give an intermediate **B** having a bridging peroxide. The optimized geometries of the models reproduce the experimental available ones (see Supporting Information). The calculated geometries of the species **A** and **B** are shown in Figure 7. The spin density of intermediate **A**, also shown, is concentrated on the O_2 ligand (O−O distance 1.289 Å, typical of O_2^-), indicating that Ti(III) has been oxidized to Ti(IV) and O_2 reduced.

Scheme 4. Gibbs Energy for Possible Reactions Leading to the Formation of $[Ti(L)Cl]_2(\mu\text{-}O)$ (3*) from $[Ti(L)Cl]$ (1*) and O_2 (L = $^{Me2}O_2NN'$; ΔG in THF, kcal·mol^{-1})[a]

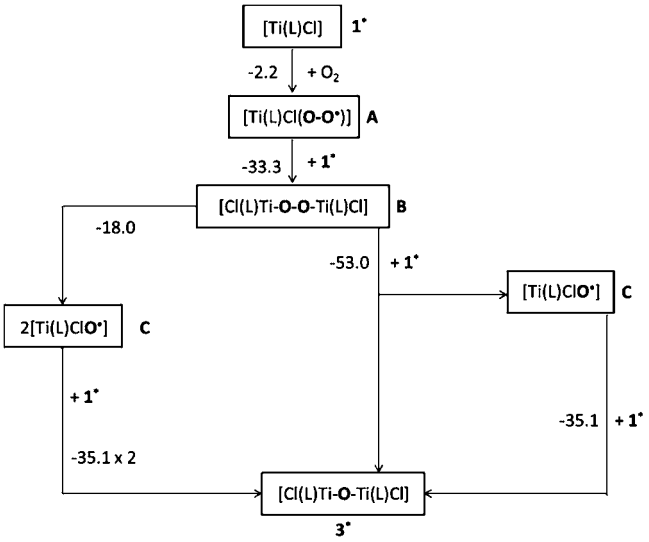

[a] **1*** and **3*** are structural models of **1** and **3**, respectively, where the *tert*-butyl groups were replaced by methyls.

The overall reaction of four moles of Ti(III) complex **1*** and 1 mol of O_2 to yield two moles of **3*** is favored by 123.6 kcal·mol^{-1} of O_2 (ΔG_{298} in THF). This result is almost the same when starting from compound **1** instead of **1***. The first step involves the coordination of O_2 to Ti(III), followed by electron transfer to afford the radical intermediate **A** (Scheme 4). This associative process is only marginally favorable ($\Delta G_{298} = -2.2$ kcal·mol^{-1}). The reaction between **A** and the reactant **1*** is more exergonic (−33.3 kcal·mol^{-1}). All together, the formation of a bridging peroxide titanium dimer from Ti(III) and O_2 is a favorable process from the thermodynamic point of view, corresponding to a global $\Delta G_{298} = -35.5$ kcal·mol^{-1}.

The peroxide dimer **B** may convert into $[Ti(L)Cl]_2(\mu\text{-}O)$, **3***, through the homolytic cleavage of the O−O bond of **B**, leading to two titanium oxido radicals (**C**) as shown on the left side of Scheme 4 ($\Delta G_{298} = -18.0$ kcal·mol^{-1}). This negative ΔG_{298} value shows that the Ti−O−O−Ti species **B** is unstable relative to the Ti−O radicals resulting from O−O cleavage. The last step of the mechanism corresponds to the formation of **3*** from the reaction of the titanium oxido radical **C** with another Ti(III) species **1***. The coupling of these two radicals is favorable by −35.1 kcal·mol^{-1}.

Alternatively, one may envisage that the cleavage of the O−O bond in **B** is assisted by Ti(III) (**1***), leading to **3*** and concomitantly to the Ti−O radical **C** (Scheme 4, center). The latter reaction corresponds to the one-electron oxidation of Ti(III) through oxygen atom transfer from **B**, a process that is reminiscent of what is commonly accepted to occur in the oxidation of organic substrates by metal peroxides. This transformation is very favorable thermodynamically ($\Delta G_{298} = -53.0$ kcal mol^{-1}). The remaining Ti−O radical **C** couples with another Ti(III) species **1*** to form **3***, as described above.

DFT calculations were also performed in order to explain the formation of the two isomers of **8** detected in the NMR. The structures of four models of complex **8**, in which the *tert*-butyl groups were replaced by methyl groups (**8***), were fully optimized. The isomer identified by X-ray diffraction, **8a***, is more stable than **8b***, the other one displaying *cis*-phenolates, by −3.5 kcal mol^{-1} (Figure 8). **8b*** must be the other isomer

dx.doi.org/10.1021/ic401008y | *Inorg. Chem.* 2013, 52, 9427−9439

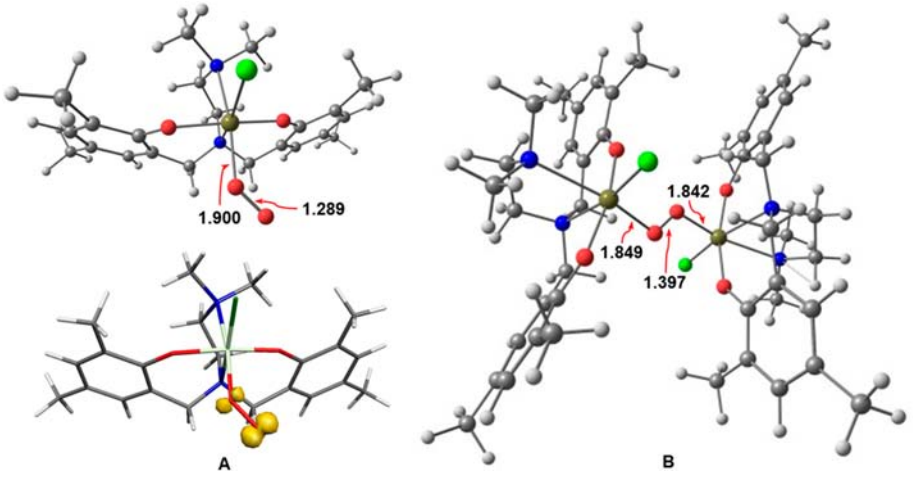

Figure 7. DFT optimized geometries of intermediates **A** (left) and **B** (right) with selected bond lengths (Å) and spin density of **A** (left, bottom).

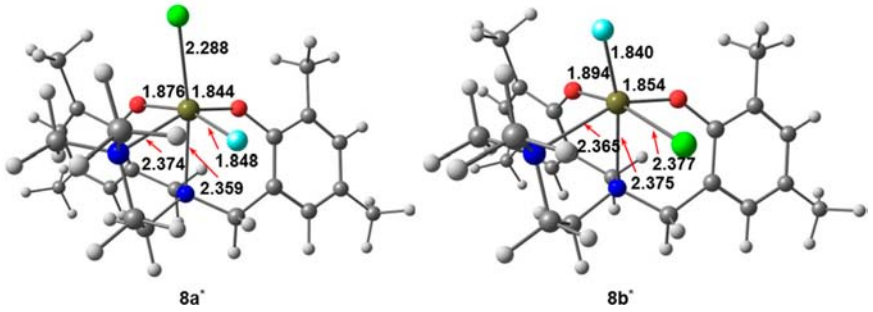

Figure 8. DFT optimized structures of **8a** (**8a***) and its isomer **8b** (**8b***), with selected bond distances (Å).

identified in the NMR spectrum because of the low symmetry. The two *trans*-phenolate isomers, **8c*** (Cl *trans* to tripodal N) and **8d*** (F *trans* to tripodal N), shown in Scheme 5, are only 1.8

Scheme 5

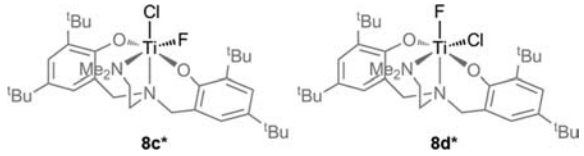

and 0.3 kcal·mol^{-1} less stable than **8a***, respectively. The small energy gaps suggest that the formation of the species displaying *cis*-phenolates (**8a*** and **8b***) is rather kinetic than thermodynamic. The approach of the PF_6^- anion to a $\{[Ti(^{tBu2}O_2NN')Cl]\}^+$ cationic species most likely occurs between one of the phenolate groups and the dimethylamine moiety (with possible decoordination) leading to a *cis*-phenolate disposition.

The Ti−F and particularly the Ti−Cl bond lengths change significantly from **8a***, the structurally characterized isomer, to **8b***, detected in solution, while the Ti−O and Ti−N bond lengths differ by much smaller amounts (Figure 8). The Ti−F and Ti−Cl distances calculated for **8a*** are in better agreement with the experimental ones determined for **8**. These results are consistent with the experimental findings as they point out for the preferential formation of one isomer, but the energy difference between them does not exclude the formation of a minor species.

In contrast, in the analogous complex $[Ti(^{tBu2}O_2NN')Cl_2]$ (**9**) with two chloride ligands, hypothetically formed from the cleavage of a dichloride bridged dication $\{[Ti(^{tBu2}O_2NN')]_2(\mu\text{-}Cl)_2\}^{2+}$, the initial *trans*-phenolates disposition is maintained. Full optimization of the two models of complex **9** (**9a***, with *trans*-phenolates, and **9b***, with *cis*-phenolates) showed that the *trans* arrangement of **9a*** is more stable, by 2.4 kcal·mol^{-1}.

Simultaneous presence of *cis*- and *trans*-phenolates was, however, observed in the cocrystal **11·12**. An isomerization process similar to the one observed in the formation of **8** may have occurred in the formation of this mixture of isomers, **11** and **12**, obtained upon exposition of the product of the oxidation of $[Ti(^{tBu2}O_2NN')(\kappa^2\text{-}\{CH_2\text{-}2\text{-}(NMe_2)\text{-}C_6H_4\})]$ (**10**) with $[FeCp_2][PF_6]$ to air.

Models of dimers **11** and **12** (**11*** and **12***), which are coordination isomers of $[Ti(^{tBu2}O_2NN')Cl]_2(\mu\text{-}O)$ (**3**) with different dispositions and coordination modes of the diamine bis(phenolate) ligand, were fully optimized. Both dimers **11*** and **12*** are less stable than **3*** by 4.8 and 13.2 kcal·mol^{-1}, respectively. These relatively small energy differences may easily be overcome by crystal packing forces acting cooperatively.

CONCLUDING REMARKS

The reactivity of titanium(III) complexes $[Ti(^{tBu2}O_2NN')Cl(S)]$ (S = THF, py) supported by a tripodal diamine bis(phenolate) ligand is described. Reactions with neutral electron acceptors as the TEMPO radical led to the formation of $[Ti(^{tBu2}O_2NN')Cl(TEMPO)]$ that displays an anionic TEMPO ligand. A similar reaction with PhN═NPh did not allow the isolation of any species displaying the azobenzene radical anion, but only a small amount of $[Ti(^{tBu2}O_2NN')Cl_2]$. This result is consistent with the occurrence of a one-electron transfer from Ti(III) to azobenzene, but given the instability of a {Ti(PhNNPh)} radical, the resulting

dx.doi.org/10.1021/ic401008y | *Inorg. Chem.* 2013, 52, 9427−9439

Ti(IV) cation rearranges to give [Ti(^{tBu2}O_2NN′)Cl_2]. Actually, the latter complex was also formed when [Ti(^{tBu2}O_2NN′)Cl(S)] was oxidized by [Cp_2Fe][BPh_4], corroborating the instability of [Ti(^{tBu2}O_2NN′)Cl]$^+$ and its tendency to convert to [Ti(^{tBu2}O_2NN′)Cl_2]. In line with this hypothesis is also the formation of [Ti(^{tBu2}O_2NN′)ClF] by fluoride abstraction from PF_6^-, upon reaction of the Ti(III) complexes with [Cp_2Fe]-[PF_6]. Contrary to all diamine bis(phenolate) compounds previously described, [Ti(^{tBu2}O_2NN′)ClF] displays *cis*-phenolate coordination. The isomer displaying the chloride ligand in the axial position, trans to the tripodal nitrogen, was identified by single crystal X-ray diffraction and shown by DFT calculations to be 3.5 kcal·mol^{-1} more stable than the complex with the fluoride ligand at the axial position.

The reactions of [Ti(^{tBu2}O_2NN′)Cl(S)] with O_2 led to [Ti(^{tBu2}O_2NN′)Cl]$_2$(μ-O). The Gibbs free energy for the reaction starting from the five coordinated intermediate [Ti(^{tBu2}O_2NN′)Cl] was calculated (DFT) as −123.6 kcal per mole of O_2. The calculations also revealed that the formation of Ti−O−Ti by reaction of the Ti−O−O−Ti core with two moles of Ti(III) is thermodynamically favored.

[Ti(^{tBu2}O_2NN′)(CH_2Ph)(S)] (S = THF, py) were obtained by chloride metathesis from [Ti(^{tBu2}O_2NN′)Cl(S)] and $PhCH_2MgCl$. The compounds are not stable in solution for long periods and, in the case of S = THF, dissociation of THF occurs readily in toluene solution. One-to-one cocrystals of [Ti(^{tBu2}O_2NN′)(CH_2Ph)$_2$] and [Ti(^{tBu2}O_2NN′)Cl]$_2$(μ-O) were grown up from a solution of [Ti(^{tBu2}O_2NN′)(CH_2Ph)(py)] in diethyl ether. The formation of the compounds most likely results from a disproportionation process of titanium(III) that results from the transfer of one benzyl radical and the abstraction of the oxygen from the solvent or traces of moisture, to generate the Ti−O−Ti moiety. These reactions take place in the presence of vestigial amounts of $MgCl_2$ that remain in the samples of [Ti(^{tBu2}O_2NN′)(CH_2Ph)(S)], if dioxane is not used to ensure its complete removal.

The oxidation of [Ti(^{tBu2}O_2NN′)(κ^2-{CH_2-2-(NMe_2)-C_6H_4})], which is a Ti(III) benzyl stabilized by the intramolecular coordination of the NMe_2 moiety, led to a complex mixture. Recrystallization of this mixture under air led to a 1:1 cocrystal of two coordination isomers of the titanium oxo dimer [Ti(^{tBu2}O_2NN′)Cl]$_2$(μ-O) differing on the coordination mode of the diamine bis(phenolate) ligands. Both molecules display C_1 symmetry and, surprisingly, in one of these dimers one metal is pentacoordinated and the other is hexacoordinated. This is the first compound where the dimethylamine moiety of the diamine bis(phenolate) ligand is not bonded to the metal. In the other complex, the coordination of the two ancillary ligands to the titanium centers reveals mutually *cis*-phenolate groups in one-half of the molecule, while they are *trans*-coordinated in the other titanium center.

This is the first systematic study on the reactivity of paramagnetic titanium(III) complexes of a nonmetallocene system. The results revealed that these species are very reactive, presenting several reaction patterns that are extremely sensitive to the experimental conditions. Cationic complexes of Ti(IV) tend to balance its extreme acidity by abstracting X type ligands or oxygen from the medium. Along with these rearrangements, the ancillary ligand may display hemilabile behavior. Although not identified in the many processes mediated by titanium diamine bis(phenolate) complexes described to date, the results reported here are relevant for the outlining of the applications of these compounds.

EXPERIMENTAL SECTION

General Procedures. All preparations and subsequent manipulations of air/moisture sensitive compounds were performed under a nitrogen atmosphere using standard Schlenk line and drybox techniques. THF, toluene, and Et_2O were dried by standard methods and distilled prior to use. C_6D_6 was dried over Na and distilled under reduced pressure. Toluene-d_8 and $CDCl_3$ were dried with 4 Å and degassed with the freeze−pump−thaw method. Unless stated otherwise, all reagents were purchased from commercial suppliers and used as received. The diamine bis(phenolate) ligand,[13f] $TiCl_3(THF)_3$,[37] and [Cp_2Fe][BPh_4][38] were prepared as described in the literature. [Ti(^{tBu2}O_2NN′)Cl(THF)] (**1**), [Ti(^{tBu2}O_2NN′)Cl(py)] (**2**), and [Ti(^{tBu2}O_2NN′)(κ^2-{CH_2-2-(NMe_2)-C_6H_4})] (**10**) were prepared as previously described.[8] The 1D and 2D (COSY, NOESY, HSQC) NMR spectra were recorded on Bruker Advance II+ 300 and 400 MHz (UltraShield Magnet) instruments at ambient temperature, unless stated otherwise. ^{1}H and ^{13}C chemical shifts (δ) are expressed in parts per million relative to Me_4Si, whereas ^{19}F and ^{31}P nuclei were referenced to external reference capillaries with CF_3COOH and H_3PO_4 (80% solution), respectively. EPR experiments were run in a Bruker EMX EPR Spectrometer and calibrated using a Perilene$^{+\bullet}$/H_2SO_4 solution as the internal standard. Carbon, hydrogen, and nitrogen analyses were performed in-house using an EA110 CE Instruments automatic analyzer. The results presented are, in general, the average of two independent determinations. Low contents of C were obtained for some low oxidation state titanium and vanadium complexes due to their extreme instability to air and moisture.

Synthetic Procedures. *[Ti(^{tBu2}O_2NN′)Cl]$_2$(μ-O), **3**.* A solution of **1** (1.40 g, 2.07 mmol) in THF was exposed to air, through a $CaCl_2$ drying tube, for 12 h. The red/orange solution obtained was evaporated to dryness, and the residue was extracted with Et_2O and filtered. Evaporation of the Et_2O solution to dryness led to an orange crystalline solid. Yield: 1.27 g, 91%. Crystals of **3** suitable for X-ray diffraction were grown from Et_2O at −20 °C and also from a C_6D_6 solution at room temperature. ^{1}H NMR (300 MHz, $CDCl_3$, ppm): δ 7.13 (d, 4H, $^4J_{HH}$ = 2.2 Hz, *p*-C*H*-Ar), 6.90 (s, 4H, $^4J_{HH}$ = 2.1 Hz, *o*-C*H*-Ar), 5.41 (d, 4H, $^2J_{HH}$ = 13.8 Hz, NCH_2Ar), 3.36 (d, 4H, $^2J_{HH}$ = 13.9 Hz, NCH_2Ar), 2.75 (m, 4H, CH_2), 2.13 (s, 12H, N(CH_3)$_2$), 1.64 (m, 4H, CH_2), 1.26 (s, 36H, C(CH_3)$_3$), 0.98 (s, 36H, C(CH_3)$_3$). ^{1}H NMR (300 MHz, C_6D_6, ppm): δ 7.47 (s, 4H, *p*-C*H*-Ar), 7.11 (s, 4H, *o*-C*H*-Ar), 5.77 (d, 4H, $^2J_{HH}$ = 13.7 Hz, NCH_2Ar), 3.30 (d, 4H, $^2J_{HH}$ = 13.8 Hz, NCH_2Ar), 2.25 (m, 4H, CH_2), 1.90 (s, 12H, N(CH_3)$_2$), 1.46 (m, 4H, CH_2), 1.44 (s, 36H, C(CH_3)$_3$), 1.36 (s, 36H, C(CH_3)$_3$). ^{13}C-{^{1}H} NMR (75 MHz, C_6D_6, ppm): δ 158.0, 138.4, 132.1, and 124.4 (C_{ipso}-Ar), 123.6 (*p*-CH−Ar), 122.3 (*o*-CH−Ar), 64.1 (NCH_2Ar), 57.6 (CH_2), 51.4 (CH_2), 48.4 (N(CH_3)$_2$), 33.1 and 32.3 (C(CH_3)$_3$), 30.0 and 29.5 (C(CH_3)$_3$). EA calculated for $C_{68}Cl_2H_{108}N_4O_5Ti_2$·2($C_4H_{10}O$): C, 66.31; H, 9.37; N, 4.07. Found: C, 66.77; H, 9.29; N, 3.66.

*[Ti(^{tBu2}O_2NN′)Cl(TEMPO)], **4**.* A solution of 2,2,6,6-tetramethylpiperidine-1-oxyl (TEMPO) (0.156 g, 1.00 mmol) in toluene was added to a solution of **1** (0.674 g, 1.00 mmol) in the same solvent at −30 °C. The temperature was allowed to rise slowly to room temperature, and the mixture was further stirred overnight. The red solution obtained was filtered, and the solvent was removed under reduced pressure leading to a red/orange crystalline solid. Yield: 0.754 g, 99%. Crystals of **4** suitable for X-ray diffraction were obtained from toluene at −20 °C. ^{1}H NMR (400 MHz, C_6D_6, ppm): δ 7.62 (d, 2H, $^4J_{HH}$ = 2.4 Hz, *p*-C*H*-Ar), 7.03 (d, 2H, $^4J_{HH}$ = 2.4 Hz, *o*-C*H*-Ar), 4.44 (d, 2H, $^2J_{HH}$ = 13.0 Hz, NCH_2Ar), 2.97 (d, 2H, $^2J_{HH}$ = 13.1 Hz, NCH_2Ar), 2.23 (m, 2H, NCH_2CH$_2$NMe$_2$), 2.12 (s, 6H, N(CH_3)$_2$), 1.79 (s, 18H, C(CH_3)$_3$), 1.59 (m, 2H, NCH$_2$CH_2NMe$_2$), 1.49 (s, 12H, CH_3-TEMPO), 1.37 (s, 18H, C(CH_3)$_3$), 1.18 (m, 4H, CH_2-TEMPO), 1.10 (m, 2H, CH_2-TEMPO). ^{13}C {^{1}H} NMR (101 MHz, C_6D_6, ppm): δ 160.2, 140.6, and 135.6 (C_{ipso}-Ar), 126.5 (CH−Ar), 125.4 (C_{ipso}-Ar), 124.7 (CH−Ar), 66.3 (NCH_2Ar), 64.3 (C_{ipso}-TEMPO), 60.3 (NCH_2CH$_2$NMe$_2$), 52.6 (NCH$_2$CH_2NMe$_2$), 51.1 (N(CH_3)$_2$), 41.0 (CH_2-TEMPO), 36.2 and 34.7 (C(CH_3)$_3$), 32.8 and 32.3 (C(CH_3)$_3$), 28.0 (br, CH_3-TEMPO), 17.0 (CH_2-TEMPO). EA calculated for $C_{43}H_{72}ClN_3O_3Ti$·0.5(C_7H_8O): C, 69.08; H, 9.47; N, 5.20. Found: C, 68.80; H, 9.54; N, 4.31.

dx.doi.org/10.1021/ic401008y | *Inorg. Chem.* 2013, 52, 9427−9439

[Ti(^{tBu2}O$_2$NN′)(CH$_2$Ph)(THF)], **5**. A 1 M solution of PhCH$_2$MgCl in Et$_2$O (1 mL, 1 mmol) was added to a solution of **1** (677 mg, 1 mmol) in toluene at −80 °C. The temperature was allowed to rise slowly to room temperature, and the mixture was further stirred overnight. The red solution obtained was evaporated to dryness, and the residue was extracted with Et$_2$O and filtered. Evaporation of the solvent to dryness led to a red crystalline solid. Yield: 325 mg, 44%. EPR (3×10^{-3} M in toluene, 293 K): $g_1 = 1.963$ (minor species), $g_2 = 1.951$ (major species).

[Ti(^{tBu2}O$_2$NN′)(CH$_2$Ph)(py)], **6**. A 1.64 M solution of PhCH$_2$MgCl in Et$_2$O (0.37 mL, 0.60 mmol) was added to a solution of **2** (411.00 mg, 0.60 mmol) in toluene at −80 °C. The temperature was allowed to rise slowly to room temperature, and the mixture was further stirred for 6 h. The purple solution obtained was evaporated to dryness, and the residue was extracted with Et$_2$O and filtered. Evaporation of the Et$_2$O solution to dryness led to a purple crystalline solid. Yield: 300 mg, 68%. Crystals of cocrystallized [Ti(^{tBu2}O$_2$NN′)Cl]$_2$(μ-O) and [Ti(^{tBu2}O$_2$NN′)-(CH$_2$Ph)$_2$] (**3·7**) suitable for X-ray diffraction were obtained from an Et$_2$O solution of [Ti(^{tBu2}O$_2$NN′)(CH$_2$Ph)(py)] at −20 °C. EPR (3×10^{-3} M in toluene, 293 K): $g = 1.952$. EA calculated for C$_{46}$H$_{66}$N$_3$O$_2$Ti·(MgCl$_2$): C, 68.06; H, 8.19; N, 5.18. Found: C, 68.32; H, 8.97; N, 5.73.

[Ti(^{tBu2}O$_2$NN′)ClF], **8**. [FeCp$_2$][PF$_6$] (0.30 g, 0.90 mmol) was added to a solution of **2** (0.62 g, 0.90 mmol) in toluene at −60 °C. The temperature was allowed to rise to room temperature, and the mixture was further stirred for 4 h. The red solution obtained was evaporated to dryness and the residue extracted with Et$_2$O. Evaporation of the Et$_2$O solution to dryness led to an orange crystalline solid. Compound **8** is obtained pure after sublimation to remove the residual ferrocene. Yield: 0.66 g, 88%. Orange crystals of **8a** suitable for X-ray diffraction were obtained from an Et$_2$O solution at −20 °C. The analysis of the NMR data revealed the presence of a minor second species, **8b**, in a relative ratio of 1:6 (coordination isomer with F$^-$ ligand *trans* to the tripodal N). **8a**: ^{1}H NMR (300 MHz, toluene−d_8, ppm): δ 7.57 (d, 1H, $^4J_{HH}$ = 2.4 Hz, *p*-C*H*-Ar), 7.41 (d, 1H, $^4J_{HH}$ = 2.3 Hz, *p*-C*H*-Ar), 7.03 (d, 1H, $^4J_{HH}$ = 2.3 Hz, *o*-C*H*-Ar), 6.65 (d, 1H, $^4J_{HH}$ = 2.3 Hz, *o*-C*H*-Ar), 4.85 (d, 1H, $^2J_{HH}$ = 13.8 Hz, NCH_2Ar), 3.98 (d, 1H, $^2J_{HH}$ = 14.0 Hz, NCH_2Ar), 2.79 (d, 1H, $^2J_{HH}$ = 13.7 Hz, NCH_2Ar), 2.71 (m, 1H, CH_2), 2.60 (m, 1H, CH_2), 2.54 (d, 1H, $^2J_{HH}$ = 14.2 Hz, NCH_2Ar), 2.49 (s, 3H, N(CH_3)$_2$), 1.93 (s, 3H, N(CH_3)$_2$), 1.83 (m, 1H, CH_2), 1.71 (s, 9H, C(CH_3)$_3$), 1.53 (s, 9H, C(CH_3)$_3$), 1.40 (m, 1H, CH_2), 1.39 (s, 9H, C(CH_3)$_3$), 1.28 (s, 9H, C(CH_3)$_3$). ^{13}C {^{1}H} NMR (75 MHz, toluene−d_8, ppm): δ 158.7, 157.3, 143.3, 142.4, 137.3, 136.8, 125.0, and 124.9 (C$_{ipso}$-Ar), 124.6, 124.5, 123.9, and 123.7 (CH−Ar), 64.6 and 61.5 (NCH_2Ar), 58.5 and 55.2 (CH_2), 52.1 and 48.3 (N(CH_3)$_2$), 36.1, 36.0, 35.0, and 34.8 (C(CH$_3$)$_3$), 32.3, 32.2, 30.9, and 30.5 (C(CH_3)$_3$). ^{19}F NMR (282 MHz, toluene-d_8, ppm): δ 190.8 (br). ^{1}H NMR (300 MHz, CDCl$_3$, ppm): δ 7.26 (d, 1H, $^4J_{HH}$ = 1.7 Hz, *p*-C*H*-Ar), 7.19 (d, 1H, $^4J_{HH}$ = 1.6 Hz, *p*-C*H*-Ar), 6.95 (s, 1H, *o*-C*H*-Ar), 6.88 (s, 1H, *o*-C*H*-Ar), 5.10 (d, 1H, $^2J_{HH}$ = 13.7 Hz, NCH_2Ar), 4.12 (d, 1H, $^2J_{HH}$ = 14.0 Hz, NCH_2Ar), 3.38 (d, 1H, $^2J_{HH}$ = 13.8 Hz, NCH_2Ar), 3.28 (m, 1H, CH$_2$CH_2NMe$_2$), 3.23 (m, 1H, CH_2CH$_2$NMe$_2$), 3.20 (d, 1H, $^2J_{HH}$ = 14.2 Hz, NCH_2Ar), 2.83 (s, 3H, N(CH_3)$_2$), 2.41 (s, 3H, N(CH_3)$_2$), 2.34 (m, 1H, CH_2CH$_2$NMe$_2$), 1.53 (s, 9H, C(CH_3)$_3$), 1.38 (s, 9H, C(CH_3)$_3$), 1.28 (m, 1H, CH$_2$CH_2NMe$_2$), 1.27 (s, 9H, C(CH_3)$_3$), 1.25 (s, 9H, C(CH_3)$_3$). ^{13}C {^{1}H} NMR (75 MHz, CDCl$_3$, ppm): δ 157.8, 156.4, 143.4, 142.6, 136.5, 135.7, 125.4, and 125.0 (C$_{ipso}$-Ar), 124.3, 124.1, 123.5, and 123.2 (CH−Ar), 64.5 and 61.6 (NCH_2Ar), 58.7 and 55.7 (CH_2), 51.9 and 48.8 (N(CH_3)$_2$), 36.0 and 35.0 (C(CH$_3$)$_3$), 32.3, 32.2, 30.9, and 30.5 (C(CH_3)$_3$). ^{19}F NMR (282 MHz, CDCl$_3$, ppm): δ 122.5 (br). **8b**: ^{19}F NMR (282 MHz, toluene-d_8, ppm): δ 164.2 (br). ^{19}F NMR (282 MHz, CDCl$_3$, ppm): δ 96.4 (br). EA calculated for C$_{34}$ClFH$_{54}$N$_2$O$_2$Ti·0.5-(C$_4$H$_{10}$O): C, 65.30; H, 8.98; N, 4.23. Found: C, 65.30; H, 9.91; N, 4.25.

[Ti(^{tBu2}O$_2$NN′)Cl$_2$], **9**. (a) Reaction of [Ti(^{tBu2}O$_2$NN′)Cl(THF)] with [FeCp$_2$][BPh$_4$]: A solution of **1** (0.358 g, 0.529 mmol) in toluene was added to a suspension of [FeCp$_2$][BPh$_4$] (0.267 g, 0.529 mmol) in toluene at −60 °C. The temperature was allowed to rise to room temperature, and the mixture was stirred overnight. The red/orange solution obtained was evaporated to dryness and the residue extracted with Et$_2$O. Evaporation of the Et$_2$O solution to dryness led to an orange solid. After sublimation to remove the residual ferrocene, **9** is the major product. Orange crystals of **9** suitable for X-ray diffraction were obtained from a C$_6$D$_6$ solution at +4 °C. (b) Reaction of [Ti(^{tBu2}O$_2$NN′)Cl(THF)] with PhNNPh: A solution of PhNNPh (0.083 g, 0.458 mmol) in toluene was added to a solution of **1** (0.310 g, 0.458 mmol) in the same solvent at −50 °C. The temperature was allowed to rise to room temperature, and the mixture was stirred overnight. The red/brown solution obtained was filtered and evaporated to dryness to give a brown powder. In toluene solution at +4 °C, an orange solid (**9**) precipitates from the brown solution. ^{1}H NMR (300 MHz, C$_6$D$_6$, ppm): δ 7.59 (d, 2H, $^4J_{HH}$ = 2.3 Hz, *p*-C*H*-Ar), 6.97 (d, 2H, $^4J_{HH}$ = 2.3 Hz, *o*-C*H*-Ar), 4.35 (d, $^2J_{HH}$ = 13.8 Hz, 2H, NCH_2Ar), 2.79 (d, $^2J_{HH}$ = 13.3 Hz, 2H, NCH_2Ar), 2.14 (m, 2H, CH_2), 1.94 (s, 6H, N(CH_3)$_2$), 1.80 (s, 18H, C(CH_3)$_3$), 1.61 (m, 2H, CH_2), 1.39 (s, 36H, C(CH_3)$_3$). ^{13}C {^{1}H} NMR (75 MHz, C$_6$D$_6$, ppm): δ 160.2, 143.6, 136.7, and 127.6 (C$_{ipso}$-Ar), 125.0 (*p*-CH−Ar), 124.4 (*o*-CH−Ar), 67.2 (NCH$_2$Ar), 60.6 (CH$_2$), 54.3 (CH$_2$), 51.3 (N(CH$_3$)$_2$), 36.1 and 35.0 (C(CH$_3$)$_3$), 32.2 and 31.4 (C(CH$_3$)$_3$).

Oxidation of [Ti(^{tBu2}O$_2$NN′)(κ^2-{CH$_2$-2-(NMe$_2$)-C$_6$H$_4$})] with [FeCp$_2$][PF$_6$]. [FeCp$_2$][PF$_6$] (94 mg, 0.28 mmol) was added to a solution of **10** (200 mg, 0.28 mmol) in toluene at −70 °C. The temperature was allowed to rise to room temperature, and the mixture was stirred for 6 h. The red solution obtained was evaporated to dryness and the residue extracted with Et$_2$O. Evaporation of the Et$_2$O solution to dryness led to a red crystalline solid. The proposed product is [Ti(^{tBu2}O$_2$NN′)(η^2-CH$_2$C$_6$H$_4$NMe$_2$)][PF$_6$]. Yield: 110 mg, 46%. ^{19}F NMR (282 MHz, C$_6$D$_6$, ppm): δ −70.69 (d, $^1J_{FP}$ = 711 Hz). ^{31}P NMR (121 MHz, C$_6$D$_6$, ppm): δ −143.0 (sept, $^1J_{PF}$ = 711 Hz). Orange crystals of two cocrystallized isomers of [Ti(^{tBu2}O$_2$NN′)Cl]$_2$(μ-O) (**11·12**) were grown from an Et$_2$O solution of the red crystalline solid exposed to air.

General Procedures for X-Ray Crystallography. Crystals suitable for single-crystal X-ray analysis were obtained for **3**, **4**, **3·7**, **8a**, and **9** as described in the synthetic procedures. Crystals of air/moisture sensitive compounds were selected inside the glovebox, covered with polyfluoroether oil, and mounted on a nylon loop. The data were collected using graphite monochromated Mo Kα radiation (λ = 0.71073 Å) on a Bruker AXS-KAPPA APEX II diffractometer equipped with an Oxford Cryosystem open-flow nitrogen cryostat. Cell parameters were retrieved using Bruker SMART software and refined using Bruker SAINT on all observed reflections. Absorption corrections were applied using SADABS.[39] The structures were solved and refined using direct methods with SIR97,[40] SIR2004,[41] or SHELXS-97[42] using the WINGX-Version 1.80.01[43] SHELXL[44] system of programs. All non-hydrogen atoms were refined anisotropically, and the hydrogen atoms were inserted in idealized positions and allowed to refine riding on the parent carbon atom. The molecular diagrams were drawn with ORTEP-3 for Windows[45] or Mercury 1.4.2,[46] included in the software package. For crystallographic experimental data and structure refinement parameters, see Table 2. Data for structures **3**, **4**, **3·7**, **8a**, and **9** were deposited in CCDC under the deposit numbers CCDC 639419 and 926866−926870 and can be obtained free of charge from The Cambridge Crystallographic Data Centre via www.ccdc.cam.uk/data_request/cif.

COMPUTATIONAL DETAILS

DFT[35] calculations for **1***, **3***, **8(a-d)***, **9**, **11**, **12**, **A**, **B**, and **C** (Me was used instead of ^{t}Bu) were performed using the Gaussian 03 software package[36] and the PBE1PBE functional, without symmetry constraints. This functional uses a hybrid generalized gradient approximation (GGA), including a 25% mixture of Hartree−Fock[47] exchange with DFT[35] exchange correlation, given by the Perdew, Burke, and Ernzerhof functional (PBE).[48] The optimized geometries were obtained with a standard 6-31G(d,p)[49] basis set for all elements (basis b1). The electronic energies obtained were converted to standard free Gibbs energies at 298.15 K by using zero point energy and thermal energy corrections based on structural and vibrational frequency data calculated at the PBE1PBE/b1 level of theory. Single point energy calculations were performed using an improved basis set (basis b2) and the geometries optimized at the PBE1BPE/b1 level. Basis b2 consisted of a standard 6-311++G(d,p).[50] Solvent effects (THF) were considered in the PBE1BPE/b2//PBE1BPE/b1 energy calculations using the polarizable continuum model (PCM) initially devised by Tomasi and co-workers[51]

dx.doi.org/10.1021/ic401008y | Inorg. Chem. 2013, 52, 9427−9439

Table 2. Selected Crystallographic Experimental Data and Structure Refinement Parameters for 3, 4, 8a, 9, 3·7, and 11·12

	3	4	8a	9	3·7	11·12
empirical formula	$C_{68}H_{108}Cl_2N_4O_5Ti_2 \cdot 2(C_4H_{10}O)$	$C_{50}H_{80}ClN_3O_3Ti$	$C_{34}H_{54}ClFN_2O_2Ti \cdot 0.5(C_4H_{10}O)$	$C_{34}H_{54}Cl_2N_2O_2Ti$	$C_{68}H_{108}Cl_2N_4O_5Ti_2 \cdot 2(C_{48}H_{68}N_2O_2Ti)$	$C_{68}H_{108}Cl_2N_4O_5Ti_2 \cdot (C_4H_{10}O)$
formula weight	1376.52	854.52	662.20	641.59	2734.17	1302.40
temperature (K)	150(2)	150(2)	150(2)	150(2)	150(2)	150(2)
crystal system	triclinic	monoclinic	monoclinic	tetragonal	triclinic	monoclinic
space group	$P\bar{1}$	$P2_1/c$	$P2_1/c$	$P4/nnc$	$P\bar{1}$	$P2/c$
a (Å)	11.505(3)	11.6720(13)	11.5340(9)	24.7045(9)	14.886(2)	35.585(4)
b (Å)	13.182(3)	25.660(3)	15.4050(13)	24.7045(9)	16.062(3)	16.471(2)
c (Å)	14.401(4)	16.9620(18)	20.717(2)	30.7712(16)	19.861(4)	26.387(3)
α (deg)	110.813(9)	90	90	90	110.793(7)	90
β (deg)	100.918(8)	93.856(5)	94.269(5)	90	100.552(7)	107.758(6)
γ (deg)	96.635(8)	90	90	90	101.118(7)	90
V (Å^3)	1964.4(9)	5068.7(10)	3670.7(6)	18780.0(14)	4189.1(12)	14729(3)
Z, ρ_{calc} (gcm^{-3})	1, 1.164	4, 1.120	4, 1.198	16, 0.908	1, 1.084	8, 1.175
μ(mm^{-1})	0.323	0.262	0.344	0.319	0.269	0.340
crystal size	0.20 × 0.20 × 0.08	0.80 × 0.20 × 0.20	0.20 × 0.10 × 0.01	0.40 × 0.40 × 0.10	0.30 × 0.10 × 0.08	0.60 × 0.30 × 0.30
crystal color	orange	orange	orange	orange	orange	orange
crystal shape	plate	needle	plate	prism	prism	block
reflns. collected	15920	89728	54863	326467	85887	163482
unique refln. [R(int)]	8024 [0.0374]	8957 [0.1524]	6940 [0.1121]	8344 [0.0769]	14437 [0.1175]	26209 [0.1329]
R1 [I > 2σ(I)]	0.0458	0.0906	0.0480	0.0694	0.0671	0.0690
wR2 [I > 2σ(I)]	0.1108	0.2115	0.0997	0.1843	0.1527	0.1614
GooF	1.053	1.109	1.001	1.084	0.943	1.033

dx.doi.org/10.1021/ic401008y | Inorg. Chem. 2013, 52, 9427−9439

as implemented in Gaussian 03.[52] The molecular cavity was based on the united atom topological model applied on UAHF radii, optimized for the HF/6-31G(d) level. Three-dimensional structures were obtained with ChemCraft[53] and the spin density with Molekel.[54]

■ ASSOCIATED CONTENT

Supporting Information

Tables with atomic coordinates of all the optimized molecules. Table with selected structural parameters for cocrystal **11·12**. X-ray crystallographic data for **3**, **4**, **3·7**, **8a**, and **9** are available as an electronic file in CIF format. This material is available free of charge via the Internet at http://pubs.acs.org.

■ AUTHOR INFORMATION

Corresponding Author

*E-mail: ana.martins@ist.utl.pt.

Notes

The authors declare no competing financial interest.

■ ACKNOWLEDGMENTS

The authors thank the Portuguese NMR Network (IST-UTL Center) for providing access to the NMR facilities and Fundação para a Ciência e a Tecnologia, Lisbon, Portugal, for funding (SFRH/BD/28762/2006, SFRH/BPD/7394/2010, PTDC/QUI/66187/2006, Pest-OE/QUI/UI0100/2011, and PEst-OE/QUI/UI0612/2013).

■ REFERENCES

(1) (a) Wichmann, O.; Sillanpaa, R.; Lehtonen, A. *Coord. Chem. Rev.* **2012**, *256*, 371−392. (b) Amgoune, A.; Thomas, C. M.; Carpentier, J.-F. *Pure Appl. Chem.* **2007**, *79*, 2013−2030. (c) Nie, K.; Fang, L.; Yao, Y.; Zhang, Y.; Shen, Q.; Y. Wang, Y. *Inorg. Chem.* **2012**, *51*, 11133−11143. (d) Maria, L.; Santos, I. C.; Alves, L. G.; Marçalo, J.; Martins, A. M. *J. Org. Chem.* **2013**, *728*, 57−67. (e) Nielson, A. J.; Telfer, S. G.; Waters, J. M. *Polyhedron* **2012**, *33*, 97−106. (f) Kapelski, A.; Buffet, J.-C.; Spaniol, T. P.; Okuda, J. *Chem. Asian J.* **2012**, *7*, 1320−1330. (g) Sauer, A.; Buffet, J.-C.; Spaniol, T. P.; Nagae, H.; Mashima, K.; Okuda, J. *Inorg. Chem.* **2012**, *51*, 5764−5770.

(2) (a) Tshuva, E. Y.; Goldberg, I.; Kol, M.; Goldschmidt, Z. *Inorg. Chem. Commun.* **2000**, *3*, 611−614. (b) Tshuva, E. Y.; Goldberg, I.; Kol, M.; Weitman, H.; Goldschmidt, Z. *Chem. Commun.* **2000**, 379−380. (c) Tshuva, E. Y.; Goldberg, I.; Kol, M.; Goldschmidt, Z. *Organometallics* **2001**, *20*, 3017−3028. (d) Groysman, S.; Tshuva, E. Y.; Goldberg, I.; Kol, M.; Goldschmidt, Z.; Shuster, M. *Organometallics* **2004**, *23*, 5291−5299.

(3) (a) Tshuva, E. Y.; Ashenhurst, J. A. *Eur. J. Inorg. Chem.* **2009**, *15*, 2203−2218. (b) Tshuva, E. Y.; Peri, D. *Coord. Chem. Rev.* **2009**, *253*, 2098−2115. (c) Dean, R. K.; Dawe, L. N.; Kozak, C. M. *Inorg. Chem.* **2012**, *51*, 9095−9103.

(4) (a) Barroso, S.; Adão, P.; Duarte, M. T.; Meetsma, A.; Pessoa, J. C.; Bouwkamp, M. W.; Martins, A. M. *Eur. J. Inorg. Chem.* **2011**, *27*, 4277−4290. (b) Segal, S.; Goldberg, I.; Kol, M. *Organometallics* **2005**, *24*, 200−202. (c) Coates, G. W.; Hustad, P. D.; Reinartz, S. *Angew. Chem., Int. Ed.* **2002**, *41*, 2236−2257. (d) Domski, G. J.; Rose, J. M.; Coates, G. W.; Bolig, A. D.; Brookhart, M. *Prog. Polym. Sci.* **2007**, *32*, 30−92.

(5) Press, K.; Cohen, A.; Goldberg, I.; Venditto, V.; Mazzeo, M.; Kol, M. *Angew. Chem., Int. Ed.* **2011**, *50*, 3529−3532.

(6) Gendler, S.; Segal, S.; Goldberg, I.; Goldschmidt, Z.; Kol, M. *Inorg. Chem.* **2006**, *45*, 4783−4790.

(7) (a) Barroso, S.; Adão, P.; Madeira, F.; Duarte, M. T.; Pessoa, J. C.; Martins, A. M. *Inorg. Chem.* **2010**, *49*, 7452−7463. (b) Madeira, F.; Barroso, S.; Namorado, S.; Reis, P. M.; Royo, B.; Martins, A. M. *Inorg. Chim. Acta* **2012**, *383*, 152−156.

(8) Barroso, S.; Cui, J.; Carretas, J. M.; Cruz, A.; Santos, I. C.; Duarte, M. T.; Telo, J. P.; Marques, N.; Martins, A. M. *Organometallics* **2009**, *28*, 3449−3458.

(9) (a) Duthaler, R. O.; Bienewald, F.; Hafner, A. Titanium-Mediated Reactions. In *Transition Metals for Organic Synthesis: Building Blocks and Fine Chemicals, Second Revised and Enlarged ed.*; Beller, M., Bolm, C., Eds.; Wiley-VCH Verlag GmbH & Co. KGaA: Weinheim, Germany, 2004; Vol. *1*, pp 491−517. (b) McMurry, J. E. *Chem. Rev.* **1989**, *89*, 1513−1524. (c) Rossi, B.; Prosperini, S.; Pastori, N.; Clerici, A.; Punta, C. *Molecules* **2012**, *17*, 14700−14732. (d) Ramón, D. J.; Yus, M. *Chem. Rev.* **2006**, *106*, 2126−2208.

(10) (a) Ephritikhine, M. *Chem. Commun.* **1998**, 2549−2554. (b) Kahn, B. E.; Rieke, R. D. *Chem. Rev.* **1988**, *88*, 733−745. (c) Gansäuer, A.; Barchuk, A.; Keller, F.; Schmitt, M.; Grimme, S.; Gerenkamp, M.; Mück-Lichtenfeld, C.; Daasbjerg, K.; Svith, H. *J. Am. Chem. Soc.* **2007**, *129*, 1359−1371. (d) Diéguez, H. R.; López, A.; Domingo, V.; Arteaga, J. F.; Dobado, J. A.; Herrador, M. M.; Del Moral, J. F. Q.; Barrero, A. F. *J. Am. Chem. Soc.* **2010**, *132*, 254−259. (e) Razus, A. C.; Dragu, E. A.; Nica, S.; Nicolescu, A. *Tetrahedron Lett.* **2011**, *52*, 1858−1862. (f) RajanBabu, T. V.; Nugent, W. A. *J. Am. Chem. Soc.* **1994**, *116*, 986−997. (g) Gansäuer, A.; Narayan, S. *Adv. Synth. Catal.* **2002**, *344*, 465−475. (h) Gansäuer, A.; Lauterbach, T.; Narayan, S. *Angew. Chem., Int. Ed.* **2003**, *42*, 5556−5573. (i) Justicia, J.; Cienfuegos, L. A.; Campaña, A. G.; Miguel, D.; Jakoby, V.; Gansäuer, A.; Cuerva, J. M. *Chem. Soc. Rev.* **2011**, *40*, 3525−3537.

(11) (a) Cuerva, J. M.; Campaña, A. G.; Justicia, J.; Rosales, A.; Oller-López, J. L.; Robles, R.; Cardenas, D. J.; Buñuel, E.; Oltra, J. E. *Angew. Chem., Int. Ed.* **2006**, *45*, 5522−5526. (b) Liu, Y.; Schwartz, J. *Tetrahedron* **1995**, *51*, 4471−4482. (c) Dosa, P.; Kronish, I.; McCallum, J.; Schwartz, J.; Barden, M. *J. Org. Chem.* **1996**, *61*, 4886−4887.

(12) (a) Agapie, T.; Diaconescu, P. L.; Mindiola, D. J.; Cummins, C. C. *Organometallics* **2002**, *21*, 1329−1340. (b) Mendiratta, A.; Cummins, C. C. *Inorg, Chem.* **2005**, *44*, 7319−7321. (c) Covert, K. T.; Wolczanski, P. T.; Hill, S. A.; Krusic, P. J. *Inorg. Chem.* **1992**, *31*, 66−78.

(13) (a) Sarazin, Y.; Howard, R. H.; Hughes, D. L.; Humphrey, S. M.; Bochmann, M. *Dalton Trans.* **2006**, 340−350. (b) Orpen, A. G.; Brammer, L.; Allen, F. H.; Kennard, O.; Watson, D. G.; Taylor, R. *J. Chem. Soc., Dalton Trans.* **1989**, *Supplement*, S1−S83. (c) Tshuva, E. Y.; Goldberg, I.; Kol, M. *Inorg. Chem.* **2001**, *40*, 4263−4270. (d) Boyd, C. L.; Toupance, T.; Tyrell, B. R.; Ward, B. D.; Wilson, C. R.; Cowley, A. R.; Mountford, P. *Organometallics* **2005**, *24*, 309−330. (e) Groysman, S.; Goldberg, I.; Kol, M.; Genizi, E.; Goldschmidt, Z. *Inorg. Chim. Acta* **2003**, *345*, 137−144. (f) Tshuva, E. Y.; Versano, M.; Goldberg, I.; Kol, M.; Weitman, H.; Goldschmidt, Z. *Inorg. Chem. Commun.* **1999**, *2*, 371−373.

(14) Nielson, A. J.; Waters, J. M. *Polyhedron* **2010**, *29*, 1715−1726.

(15) (a) Kuhn, N.; Maichle-Mößmer, C.; Weyers, G. *Anorg. Allg. Chem.* **1999**, *625*, 851−856. (b) Babcock, L. M.; Klemperer, W. G. *Inorg. Chem.* **1989**, *28*, 2003−2007. (c) Varkey, S. P.; Schormann, M.; Pape, T.; Roesky, H. W.; Noltemeyer, M.; Herbst-Irmer, R.; Schmidt, H. G. *Inorg. Chem.* **2001**, *40*, 2427−2429. (d) Bieller, S.; Bolte, M.; Lerner, H. W.; Wagner, M. *Inorg. Chem.* **2005**, *44*, 9489−9496. (e) Peri, D.; Meker, S.; Shavit, M.; Tshuva, E. Y. *Chem.—Eur. J.* **2009**, *15*, 2403−2415. (f) Roesky, H. W.; Haiduc, I.; Hosmane, N. S. *Chem. Rev.* **2003**, *103*, 2579−2595.

(16) Newhouse, T. R.; Li, X.; Blewett, M. M.; Whitehead, C. M. C.; Corey, E. J. *J. Am. Chem. Soc.* **2012**, *134*, 17354−17357.

(17) (a) Ward, A. L.; Elbaz, L.; Kerr, J. B.; Arnold, J. *Inorg. Chem.* **2012**, *51*, 4694−4706. (b) Bould, J.; Base, T.; Londesborough, M. G. S.; Oro, L. A.; Macías, R.; Kennedy, J. D.; Kubát, P.; Fuciman, M.; Polívka, T.; Lang, K. *Inorg. Chem.* **2011**, *50*, 7511−7523.

(18) Nakamura, R.; Nakato, Y. *J. Am. Chem. Soc.* **2004**, *126*, 1290−1298.

(19) Tyeklar, Z.; Jacobson, R. R.; Wei, N.; Murthy, N. N.; Zubieta, J.; Karlin, K. D. *J. Am. Chem. Soc.* **1993**, *115*, 2677−2689.

(20) (a) Mazzanti, M.; Rosset, J.-M.; Floriani, C.; Chiesi-Villa, A.; Guastini, A. *J. Chem. Soc., Dalton Trans.* **1989**, 953−957. (b) Boro, B. J.; Lansing, R.; Goldberg, K. I.; Kemp, R. A. *Inorg. Chem. Commun.* **2011**, *14*, 531−533.

(21) (a) Matsumoto, K.; Feng, C.; Handa, S.; Oguma, T.; Katsuki, T. *Tetrahedron* **2011**, *67*, 6474−6478. (b) Ventura, M.; Mosquera, M. E.

G.; Cuenca, T.; Royo, B.; Jiménez, G. *Inorg. Chem.* **2012**, *51*, 6345−6349. (c) Mba, M.; Prins, L. J.; Zonta, C.; Cametti, M.; Valkonen, A.; Rissanen, K.; Licini, G. *Dalton Trans.* **2010**, *39*, 7384−7392. (d) Adão, P.; Avecilla, F.; Bonchio, M.; Carraro, M.; Pessoa, J. C.; Correira, I. *Eur. J. Inorg. Chem.* **2010**, 5568−5578. (e) Wang, Y.; Wang, M.; Wang, L.; Wang, Y.; Wang, X.; Sun, L. *Appl. Organomet. Chem.* **2011**, *25*, 325−330.

(22) (a) Bauer, D. P.; Macomber, R. S. *Inorg. Chem.* **1976**, *15*, 1985−1986. (b) Boche, G.; Möbus, K.; Harms, K.; Marsch, M. *J. Am. Chem. Soc.* **1996**, *118*, 2770−2771. (c) DiPasquale, A. G.; Hrovat, D. A.; Mayer, J. M. *Organometallics* **2006**, *25*, 915−924. (d) Kondo, S.; Saruhashi, K.; Seki, K.; Matsubara, K.; Miyaji, K.; Kubo, T.; Matsumoto, K.; Katsuki, T. *Angew. Chem., Int. Ed.* **2008**, *47*, 10195−10198.

(23) (a) Mahanthappa, M. K.; Huang, K.-W.; Cole, A. P.; Waymouth, R. M. *Chem. Commun.* **2002**, 502−503. (b) Huang, K.-W.; Waymouth, R. M. *J. Am. Chem. Soc.* **2002**, *124*, 8200−8201. (c) Mahanthappa, M. K.; Cole, A. P.; Waymouth, R. M. *Organometallics* **2004**, *23*, 836−845. (d) Schröder, K.; Haase, D.; Saak, W.; Beckhaus, R.; Kretschmer, W. P.; Lützen, A. *Organometallics* **2008**, *27*, 1859−1868.

(24) Gyepes, R.; Varga, V.; Horáček, M.; Kubišta, J.; Pinkas, J.; Mach, K. *Organometallics* **2010**, *29*, 3780−3789.

(25) Huang, K.-W.; Han, J. H.; Cole, A. P.; Musgrave, C. B.; Waymouth, R. M. *J. Am. Chem. Soc.* **2005**, *127*, 3807−3816.

(26) (a) Steffey, B. D.; Fanwick, P. E.; Rothwell, I. P. *Polyhedron* **1990**, *9*, 963−968. (b) Willis, C. J. *Coord. Chem. Rev.* **1988**, *88*, 133−202. (c) Nielson, A. J.; Schwerdtfeger, P.; Waters, J. M. *J. Chem. Soc., Dalton Trans.* **2000**, 529−537.

(27) Enemrke, R. J.; Larsen, J.; Skrydstrup, T.; Daasbjerg, K. *J. Am. Chem. Soc.* **2004**, *126*, 7853−7864.

(28) (a) Thorman, J. L.; Young, V. G.; Boyd, P. D. W.; Guzei, I. A.; Woo, L. K. *Inorg. Chem.* **2001**, *40*, 499−506. (b) Hill, J. E.; Profilet, R. D.; Fanwick, P. E.; Rothwell, I. P. *Angew. Chem., Int. Ed. Engl.* **1990**, *29*, 664−665. (c) Bogdanovic, B.; Bolte, A. *J. Organomet. Chem.* **1995**, *502*, 109−121. (d) Aleandri, L. E.; Bogdanovic, B.; Gaidies, A.; Jones, D. J.; Liao, S.; Michalowicz, A.; Rozière, J.; Schott, A. *J. Organomet. Chem.* **1993**, *459*, 87−93.

(29) (a) Solari, E.; Angelis, S. D.; Floriani, C.; Chiesi-Villa, A.; Rizzoli, C. *Inorg. Chem.* **1992**, *31*, 96−101. (b) Rosset, J.-M.; Floriani, C.; Mazzanti, M.; Chiesi-Villa, A.; Guastini, C. *Inorg. Chem.* **1990**, *29*, 3991−3996. (c) Ejfler, J.; Szafert, S.; Sobota, P. *Macromol. Symp.* **2010**, *296*, 77−79.

(30) Sarazin, Y.; Howard, R. H.; Hughes, D. L.; Humphrey, S. M.; Bochmann, M. *Dalton Trans.* **2006**, 340−350.

(31) (a) Handa, Y.; Inanaga, J. *Tetrahedron Lett.* **1987**, *28*, 5717−5718. (b) Green, M. L. H.; Lucas, C. R. *Dalton Trans.* **1972**, 1000−1003. (c) Sekutowski, D.; Jungst, R.; Stucky, G. D. *Inorg. Chem.* **1978**, *17*, 1848−1855. (d) Stephan, D. W. *Organometallics* **1992**, *11*, 996−999.

(32) (a) Jordan, R. F.; Dasher, W. E.; Echols, S. F. *J. Am. Chem. Soc.* **1986**, *108*, 1718−1719. (b) Ferreira, M. J.; Matos, I.; Ascenso, J. R.; Duarte, M. T.; Marques, M. M.; Wilson, C.; Martins, A. M. *Organometallics* **2007**, *26*, 119−127.

(33) (a) Bodner, A.; Jeske, P.; Weyhermuller, T.; Wieghardt, K.; Dubler, E.; Schmalle, H.; Nuber, B. *Inorg. Chem.* **1992**, *31*, 3737−3748. (b) Shah, S. A. A.; Dorn, H.; Gindl, J.; Noltemeyer, M.; Schmidt, H.-G.; Roesky, H. W. *J. Organomet. Chem.* **1998**, *550*, 1−6. (c) Taw, F.; Scott, B. L.; Kiplinger, J. L. *J. Am. Chem. Soc.* **2003**, *125*, 14712−14713.

(34) (a) Clarkson, G. J.; Gibson, V. C.; Goh, P. K. Y.; Hammond, M. L.; Knight, P. D.; Scott, P.; Smit, T. M.; White, A. J. P.; Williams, D. J. *Dalton Trans.* **2006**, 5484−5491. (b) Blackmore, K. J.; Lal, N.; Ziller, J. W.; Heyduk, A. F. *Eur. J. Inorg. Chem.* **2009**, 735−743. (c) Saito, J.; Mitani, M.; Matsui, S.; Tohi, Y.; Makio, H.; Nakano, T.; Tanaka, H.; Kashiwa, N.; Fujita, T. *Macromol. Chem. Phys.* **2002**, *203*, 59−65.

(35) Parr, R. G.; Young, W. In *Density Functional Theory of Atoms and Molecules*; Oxford University Press: New York, 1989.

(36) Frisch, M. J.; Trucks, G. W.; Schlegel, H. B.; Scuseria, G. E.; Robb, M. A.; Cheeseman, J. R.; Montgomery, J. A., Jr.; Vreven, T.; Kudin, K. N.; Burant, J. C.; Millam, J. M.; Iyengar, S. S.; Tomasi, J.; Barone, V.; Mennucci, B.; Cossi, M.; Scalmani, G.; Rega, N.; Petersson, G. A.; Nakatsuji, H.; Hada, M.; Ehara, M.; Toyota, K.; Fukuda, R.; Hasegawa, J.; Ishida, M.; Nakajima, T.; Honda, Y.; Kitao, O.; Nakai, H.; Klene, M.; Li, X.; Knox, J. E.; Hratchian, H. P.; Cross, J. B.; Adamo, C.; Jaramillo, J.; Gomperts, R.; Stratmann, R. E.; Yazyev, O.; Austin, A. J.; Cammi, R.; Pomelli, C.; Ochterski, J. W.; Ayala, P. Y.; Morokuma, K.; Voth, G. A.; Salvador, P.; Dannenberg, J. J.; Zakrzewski, V. G.; Dapprich, S.; Daniels, A. D.; Strain, M. C.; Farkas, O.; Malick, D. K.; Rabuck, A. D.; Raghavachari, K.; Foresman, J. B.; Ortiz, J. V.; Cui, Q.; Baboul, A. G.; Clifford, S.; Cioslowski, J.; Stefanov, B. B.; Liu, G.; Liashenko, A.; Piskorz, P.; Komaromi, I.; Martin, R. L.; Fox, D. J.; Keith, T.; M. A. Al-Laham, Peng, C. Y.; Nanayakkara, A.; Challacombe, M.; Gill, P. M. W.; Johnson, B.; Chen, W.; Wong, M. W.; Gonzalez, C.; Pople, J. A. *Gaussian 03*, revision C.02; Gaussian, Inc.: Wallingford, CT, 2004.

(37) Manzer, L. E. *Inorg. Synth.* **1982**, *21*, 135−140.

(38) Jordan, R. F.; LaPointe, R. E.; Bradley, P. K.; Baenziger, N. *Organometallics* **1989**, *8*, 2892−2903.

(39) Sheldrick, G. M. *SADABS, Program for Empirical Absorption Correction*; University of Göttingen: Göttingen, Germany, 1996.

(40) Altomare, A.; Burla, M. C.; Camalli, M.; Cascarano, G. L.; Giacovazzo, C.; Guagliardi, A.; Moliterni, A. G. G.; Polidori, G.; Spagna, R. *J. Appl. Crystallogr.* **1999**, *32*, 115−119.

(41) Burla, M. C.; Caliandro, R.; Camalli, M.; Carrozzini, B.; Cascarano, G. L.; De Caro, L.; Giacovazzo, C.; Polidori, G.; Spagna, R. *J. Appl. Crystallogr.* **2005**, *38*, 381−388.

(42) Sheldrick, G. M. *Acta Crystallogr.* **1990**, *A46*, 467−473.

(43) Farrugia, L. J. *J. Appl. Crystallogr.* **1999**, *32*, 837−838.

(44) (a) Sheldrick, G. M. *SHELXL-97*, release 97−2; University of Göttingen: Göttingen, Germany, 1998. (b) Sheldrick, G. M. *Acta Crystallogr.* **2008**, *A64*, 112−122.

(45) Farrugia, L. J. *J. Appl. Crystallogr.* **1997**, *30*, 565−566.

(46) Macrae, C. F.; Edgington, P. R.; McCabe, P.; Pidcock, E.; Shields, G. P.; Taylor, R.; Towler, M.; van de Streek, J. *J. Appl. Crystallogr.* **2006**, *39*, 453−457.

(47) Hehre, W. J.; Radom, L.; Schleyer, P. V. R.; Pople, J. A. In *Ab Initio Molecular Orbital Theory*; John Wiley & Sons: New York, 1986.

(48) (a) Perdew, J. P.; Burke, K.; Ernzerhof, M. *Phys. Rev. Lett.* **1997**, *78*, 1396. (b) Perdew, J. P. *Phys. Rev. B* **1986**, *33*, 8822−8824.

(49) (a) Ditchfield, R.; Hehre, W. J.; Pople, J. A. *J. Chem. Phys.* **1971**, *54*, 724−728. (b) Hehre, W. J.; Ditchfield, R.; Pople, J. A. *J. Chem. Phys.* **1972**, *56*, 2257−2261. (c) Hariharan, P. C.; Pople, J. A. *Mol. Phys.* **1974**, *27*, 209−214. (d) Gordon, M. S. *Chem. Phys. Lett.* **1980**, *76*, 163−168. (e) Hariharan, P. C.; Pople, J. A. *Theor. Chim. Acta* **1973**, *28*, 213−222.

(50) (a) McClean, A. D.; Chandler, G. S. *J. Chem. Phys.* **1980**, *72*, 5639−5648. (b) Krishnan, R.; Binkley, J. S.; Seeger, R.; Pople, J. A. *J. Chem. Phys.* **1980**, *72*, 650−654. (c) Wachters, A. J. H. *J. Chem. Phys.* **1970**, *52*, 1033−1037. (d) Hay, P. J. *J. Chem. Phys.* **1977**, *66*, 4377−4384. (e) Raghavachari, K.; Trucks, G. W. *J. Chem. Phys.* **1989**, *91*, 1062−1065. (f) Binning, R. C., Jr.; Curtis, L. A. *J. Comput. Chem.* **1990**, *11*, 1206−1216. (g) McGrath, M. P.; Radom, L. *J. Chem. Phys.* **1991**, *94*, 511−516. (h) Clark, T.; Chandrasekhar, J.; Spitznagel, G. W.; von, P.; Scheleyer, R. *J. Comput. Chem.* **1983**, *4*, 294−301. (i) Frisch, M. J.; Pople, J. A.; Binkley, J. S. *J. Chem. Phys.* **1984**, *80*, 3265−3269.

(51) (a) Cancès, E.; Mennucci, B.; Tomasi, J. *J. Chem. Phys.* **1997**, *107*, 3032−3041. (b) Cossi, M.; Barone, V.; Mennucci, B.; Tomasi, J. *Chem. Phys. Lett.* **1998**, *286*, 253−260. (c) Mennucci, B.; Tomasi, J. *J. Chem. Phys.* **1997**, *106*, 5151−5158.

(52) (a) Tomasi, J.; Mennucci, B.; Cammi, R. *Chem. Rev.* **2005**, *105*, 2999−3094. (b) Cossi, M.; Scalmani, G.; Rega, N.; Barone, V. *J. Chem. Phys.* **2002**, *117*, 43−54.

(53) ChemCraft. http://www.chemcraftprog.com/index.html.

(54) Portmann, S.; Lüthi, H. P. *Chimia* **2000**, *54*, 766−770.